CONTROL ELECTRONICS FOR PRECISION MEASUREMENT OF ULTRA COLD ATOMS

Thesis submitted in partial fulfillment for the degree of

M.Sc. (Engg.) by Research
in
Electronics Engineering
of
VISVESVARAYA TECHNOLOGICAL UNIVERSITY
Belgaum, India

by
MEENA M S
(USN: 1BM08MEM01)

Under the guidance of
Dr. B.KANMANI
Professor

Research Center
Department of Telecommunication Engineering
B.M.S. College of Engineering
Bangalore-560038, Karnataka, India

Feb 2013

CONTROL ELECTRONICS FOR PRECISION MEASUREMENT OF ULTRA COLD ATOMS

Thesis submitted for the award of degree
of
M.Sc. (Engg.) by Research
(Electronics Engineering)
by

MEENA M S
(USN: 1BM08MEM01)

VISVESVARAYA TECHNOLOGICAL UNIVERSITY
BELGAUM-560 018

Research Center
Department of Telecommunication Engineering
B.M.S. College of Engineering
Bangalore-560019, Karnataka, India

February 2013

Research Center

DEPARTMENT OF TELE-COMMUNICATION ENGINEERING
B.M.S. COLLEGE OF ENGINEERING
BANGALORE – 560019

CERTIFICATE

Certified that the thesis entitles, "**Control Electronics for Precision Measurement of Ultra Cold Atoms"** is carried out by**Mrs. Meena M. S.**, a bonafide student of B.M.S. College of Engineering, Bangalore,in partial fulfillment for the award of **M.Sc. (Engg.) by Research** in **Electronics Engineering**of Visvesvaraya Technological University, Belgaum, during the years 2008-2013.

To the best of my knowledge, the work reported in the thesis has not been submitted byme elsewhere for the award and is not a repetition of the work carried out by others.

Meena M. S.
(Candidate)

To the best of our knowledge, the above statement made by the candidate, MeenaM.S.(USN: 1BM08MEM01) is true.

Dr. B. Kanmani(Guide)
Professor and HOD
Department of Telecommunication Engineering,
BMS College of Engineering,
Bangalore-560 019.

Dr. Andal Narayanan (Co-guide)
Asst Professor, LAMP Group
Raman Research Institute
Sadashivnagar,
Bangalore-560080

Dr. MallikharjunaBabu
Principal
B.M.S. College of Engineering,
Bangalore-560 019

ABSTRACT

Laser cooling and atom trapping is an interesting and challenging field of physics, where in a group of atoms (e.g. Rubidum, Cesium, Pottasium) are cooled down to few orders of micro Kelvin temperatures using Laser sources. The interaction between light and atoms has given the way to modern atom optics and its application in research & industry. Many different laser cooling and trapping mechanisms have been demonstrated and more atomic species have been laser cooled.

Laser cooled atoms are used to study the atom light interaction in general and serve as cold atom sources for other experiments like Bose-Einstein condensation, atom interferometry, collision studies and metrology like precision measurements of time & frequency, and fundamental constants.Tunable diode lasers are widely used in atomic physics. The main advantages of the diode lasers are the low cost, small size, sufficient laser power output, wide wavelength range and tunability. Important requirements of Laser cooling and atom trapping experiment are Stable Laser sources, precision electronics and instrumentation, Image acquisition systems and automation of experiments which involves interfacing the testing and measuring equipments.

This project work aims towards achieving some of the requirements of the Laser cooling and atom trapping experiments. Chapter 1 gives the introduction and overview of the project. Chapter 2 gives the details of diode lasers and External Cavity Diode Laser (ECDL) and associated electronic circuit and module details to achieve a narrow line width laser source which is locked to a hyper fine transition of Rubidium atoms. In many applications the original laser frequency (at 10^ {14} Hz) has to be shifted by a few hundred MHz using AOMs (Acousto-Optic Modulators). Chapter 3 describes the PI based feedback mechanism locking techniques to lock the AOM frequency and followed by the results of the setup.

In laser cooling experiments to trap the atoms in a Magneto Optical trap (MOT), a pair of Anti- Helmholtz magnetic coil is used to produce the required magnetic field gradients. To capture the atoms and for characterising the MOT it is essential to switch on and off the

MOT. Chapter 4 describes IGBT based switching circuits for magnetic coil switching and Lock-in detection techniques for temperature measurement of the cooled and trapped atoms, and concluded by the results of the circuits.

Light matter interactions are studied in samples of single atom and single photon. To achieve single atoms Rubidium 87 atoms are laser cooled in a Magneto Optic Trap, and transferred to a magnetic trap. Detection of trapped atoms is usually is done by illuminating the trap with a near resonant laser, and fluorescence is measured. Light matter interactions are studied by detecting the photons and obtaining the statistics of the arrival times of photon distribution**.** Chapter 5 describes the details of the electronics circuits and modules to achieve single atom detection and results of the modules.

Meena M.S.

ACKNOWLEDGEMENT

It is with immense sense of gratitude I place on record my indebtness to my guide Dr. B. Kanmani, HOD, Tele- communication department, BMS college of Engineering under whose expert guidance carried out this work.

I am thankful to my co-guide Dr. Andal Narayanan, Asst Professor, Raman Research Institute, Bangalore for her continuing support, timely suggestions and valuable help for the successful completion of this work.

I am very much thankful to Dr. Ravi Subramanian, Director, RRI for the facilities provided at RRI to do my project work.

I am very thankful to Dr. Hema Ramachandran, HRF, LAMP group, RRI, for he encouragement and for the guidance.

I am thankful to Nandan Sathpathy, Deepak Pandey, PhD students at RRI for their continuous interactions, help and timely suggestions.

A special note of thanks goes to Ashwin, Shafi, Girish , Dhana, Asha, Amrutha, all my Lab mates, RAL staff and workshop staff for their help.

Finally I express my deep gratitude to my family for their encouragement and prayers.

NOMENCLATURE

ADC	Analog to Digital Converter
AOM	Acousto-Optic Modulator
Ca	Calcium
CCD	Charge coupled Device
CMRR	Common Mode Rejection Ratio
Cs	Cesium
DAC	Digital to Analog Converter
EMF	Electro Motive Force
FM	Frequency Modulation
FSK	Frequency Shift Keying
GHz	Giga Hertz
LVDS	Low voltage Diffierential Signalling
Li	Lithium
mA	milli ampere
m bar	milli bar
mm	milli metre
mH	milli Henry
mW	milli watt
MHz	Mega Hertz
MOT	Magneto Optic Trap
nh	nano Henry
Na	Sodium
PSD	Phase Sensitive Detection
Rb	Rubidium
S.D.	Standard Deviation
Torr	Unit of pressure
µK	micro Kelvin
VCO	Voltage Controlled Oscillator

TABLE OF CONTENTS

LIST OF FIGURES

Chapter 1

1.1. Introduction

Laser cooling and atom trapping lab in Raman Research Institute is aiming towards fundamental study of the laser cooled atoms in a trap. The control of atomic motion by laser light is an application that has exploded over the last few years. The possibility of reaching extremely low atomic kinetic-energy temperatures near absolute zero is astonishing achievement. Research in atom trapping and cooling has led to insights into the interaction of matter and radiation and a variety of applications in areas such as spectroscopy, atomic clocks, atomic interferometers, optical lithography, and gravitational measurements.

Laser beams are used to cool atoms and trap them in space. This technique has readily been demonstrated first by the Nobel prize-winning work of Steven Chu, William D. Phillips and Claude Cohen-Tannoudji. When an atom is illuminated by counter-propagating light and absorbs a photon, its momentum changes the atomic velocity. After many cycles of absorption and emission, the velocity of the atom becomes nearly zero. In each cycle the atom loses energy which corresponds to the Doppler shift. The kinetic energy of the atom can eventually be lower than one micro Kelvin. This atom can then be trapped by two opposing laser beams that have frequencies lower than the atom's absorption maximum. As the atom moves in the direction of one of the laser beams it sees a frequency increase (Doppler effect). The frequency increase moves into the atom's absorption band causing a momentum kick in the opposite direction. The atom is then fixed in space by the two beams. Cooling allows the atom to be held longer since its random thermal motions are minimized.

Tunable diode lasers are widely used in atomic physics. The main advantages of the diode lasers are the low cost, small size, sufficient laser power output, wide wavelength range and tunability. These lasers are used in laser printer, CD player, bar code scanner and in optical communications also. The available wavelength range of diode lasers cover atomic transitions of many inorganic atoms such as Li,Na,Rb,Cs and Ca. In particular the laser output is some tens of MHz wide and can be continuously tuned only over cer-

tain limited region. These characteristics can be improved by the use of optical feedback to control the laser. To achieve this, Laser diode is placed in an External Cavity Diode Laser (ECDL), to achieve laser sources stable up to few MHz. The components of an ECDL, Temperature stabilization circuits and Frequency Locking Techniques have been discussed.

Commercial lasers used in these experiments employ sophisticated feedback mechanism to maintain the laser frequency to the desired accuracy. In many applications the original laser frequency (at 10^{14} Hz) has to be shifted by a few hundred MHz using Acousto Optic modulators (AOM). It uses the acousto-optic effect to diffract and shift the frequency of light using sound waves (usually at radio-frequency). A piezoelectric transducer is attached to a material such as glass. An oscillating electric signal drives the transducer to vibrate, which creates sound waves in the glass. These can be thought of as moving periodic planes of expansion and compression that change the index of refraction. Incoming light scatters off the resulting periodic index modulation and interference occurs. The output RF frequency of an AOM, drifts from its initial set value due to AOM crystal getting heated up, and due to fluctuations in the driving voltages. A feedback mechanism to control such changes in the frequency of the RF output produced by the AOM driver is developed, which corrects for the frequency change by changing the AOM tuning voltage. To this end a PI based feedback mechanism is developed to control any error produced due to the shift in the RF output, which is detected and relevant control action is taken by sending a feedback signal back to the AOM.

Trapping and cooling of atoms can be achieved using the interaction between the atomic magnetic moment and the magnetic field. The MOT (Magneto Optic Trap) has proven to be an extremely versatile laboratory tool which can be constructed with reasonable ease. The magnetic field gradients needed (~12 G/cm) are well within the limits attainable by standard Helmholtz coils operating at reasonable currents (e.g. 200 turns with 3 Amp). The addition of the anti-Helmholtz coils to the set-up provides a spherical, quadrupole magnetic field, arranged so that the zero of the field is at the trap centre. The field increases approximately linearly as one extends outwards from the zero region, along the symmetry axis of the coils. Temperatures in the μK range are achieved using

magneto-optical trapping. Magnetic trapping is created by adding a spatially-varying magnetic field to the optical field used for laser cooling, driving the atoms to the centre. To capture the atoms, the magnetic field needs to be switched on. For characterising the MOT, i.e. to calculate number of atoms, decay rate etc, it is essential to switch off the MOT. Most of the measurements are made after the magnetic field is switched off, i.e. during the decay time. In this regard IGBT (Mitsubishi) based switching system is developed which switches the magnetic coils on and off at currents up to 5A, up to 100 Hz. IGBT based system includes driver circuitry for IGBT, snubber circuit for protections purposes, and freewheeling circuitry for back emf suppressions. In the experimental setup to achieve the required results the entire experiment needs to be automated. Each experiment has a particular sequence in which devices like shutters, AOMs etc has to be switched on/off and Magnetic coil currents has to be varied. The currents in magnetic coils need to be ramped up and down in time intervals of few milliseconds. Data Acquisition systems from National Instruments and LabVIEW programs are designed, developed and implemented to automate the experiments for switching the magnetic coils on/off and for ramping the currents in the magnetic coils.

Cold atoms produced by laser cooling and trapping techniques are used widely for different high precision experiments like high resolution spectroscopy, precision measurements, accurate atomic clocks, quantum information, quantum entanglement of atoms, single atom traps etc. Thus, to perform such highly precise experiments with cold atoms one needs an accurate characterization of the cold atoms. Temperature of the cold atoms is a very essential characteristic physical quantity which is very useful in performing such accurate experiments. To measure the temperature of the Magneto Optic Trap (MOT), Lock-in detection based technique known as Trap Oscillation method is designed and implemented. In this technique an additional pair of magnetic coils are used, which are driven by a Power amplifier (OPA 541) to introduce oscillating magnetic field. This oscillating magnetic field causes the cold atom cloud to oscillate, which is detected by a Photo detector. Lock-in detection techniques are used to measure the phase difference (Ø) between the reference signal and the detector signal. By measuring the phase difference (Ø), at different frequencies of the oscillating magnetic field, the temperature of the cold cloud is evaluated as 260 μ Kelvin.

Submitted by Meena M S, USN:1BM08MEM01

Light matter interactions are studied in samples of single atom and single photon. To achieve single atoms Rubidium 87 atoms are laser cooled in a Magneto Optic Trap, and transferred to a magnetic trap. Detection of trapped atoms is usually is done by illuminating the trap with a near resonant laser, and fluorescence is measured. Light matter interactions are studied by detecting the photons and obtaining the statistics of the arrival times of photon distribution.

In our experiments to detect single photons we are using single photon counting module SPCM-AQR-14 from Perkin Elmer. For counting single photons, FPGA based Detection system is used. It is a Virtex-5 board, which has a 125MHz onboard clock. FPGA board is designed to accept Differential signalling – LVDS (Low voltage differential signalling). A level translator card is required as interface between SPCM which gives out TTL signals and FPGA system which accepts differential signals. To achieve this level translator card using IC DS90LV019, is designed and implemented, which is a Driver/Receiver designed specifically for the high speed low power point-to-point interconnect applications.

In single atom experiments two Avalanche Photo Detectors (APD) will be used to study the coincidence counting. In this process we have to vary or introduce the delay (up to-few ns) in one of the Gating trigger signals given the APD. To achieve a module having a Coarse Delay circuit- which introduces delay in steps of 10ns and a Variable delay circuit – 0 -10 ns variable delay is designed, tested and implemented.

1.2 Scope of the Present Study

For Laser cooling and atom trapping experiments important requirements are Stable Laser sources, precision electronics and instrumentation, Image acquisition systems and automation of experiments which involves interfacing the testing and measuring equipments. The time scales involved in these experiments are from few orders of micro seconds to milli seconds.

To achieve the aims and results in these experiments which are complex, high precision electronic circuits and instrumentation is required in all stages of the experiments. This project report aim towards designing, building instrumentation and automation of the experiments as per the requirements of the experiments in the labs at Raman Research Institute.

1.3 Objectives

The main objectives of the present project work are:

1. Design and build a PI based Controller for frequency control of an Acousto-Optic Modular (AOM), which is used to shift laser light frequencies by few tens of MHz.

2. Design a IGBT based switching circuit for the magnetic coils in a Magneto-Optic Trap at 5A current, up to 100 Hz.

3. Develop a Data Acquisition system (DAQ) for automating the experiments based on LabVIEW to interface the Agilent programmable power supply and Magnetic coil switching circuits.
4. Design and implement a Power amplifier based circuit for oscillating the cold cloud and implement Lock-in detection techniques for the "Trap oscillation method " to measure the temperature of the cold cloud .
5. Design and implement Level Translator card (TTL to LVDS) for FPGA based data acquisition system used for Single atom experiments, Coarse Delay and Variable Delay circuits to introduce delay in order of few ns to gate trigger signals for Single Photon Avalanche Detectors (SPAD).

Chapter 2: Physics information

2.1. Laser cooling and Trapping

Frequency stabilized laser diodes are used in various applications in atomic physics. Lasers with combination of high power, small line-width and fast tunability are essential for many areas in high resolution spectroscopy. One example is the fascinating field of laser atom cooling and trapping. Laser cooling is a method of using lasers to cool gases to micro Kelvin range. Requirements for a laser system used in this field for various applications are extensive: a mode hop free tuning range of a few GHz, with a line-width in the regime of 1MHz with an output power of few hundreds of mW.

In the Laser cooling and trapping experiments the laser frequency has to be stabilized to either the side of or to the peak of any sufficiently well resolved transition of the Rubidium (or any other alkali element being used in the experiment) hyperfine absorption spectrum. We have chosen Rubidium. Rubidium is a convenient atom to study with absorption spectroscopy, because it has a single electron outside of closed shells, it has relatively simple structure of energy levels like hydrogen.

More importantly, the wavelength of the operation of Rubidium is 780 nm. Diode Lasers operating at 780nm are readily available. With output frequency stabilized against atomic transition frequency through saturated absorption, these diode lasers can be a very effective laser source for many high precision atomic physics experiments.

The basic idea used in laser cooling is that photons, can impart their momentum on to the atoms they interact. Atoms heading towards the laser are slowed as they are bombarded by photons. After cooling, the atoms have to be retained in a confined region long enough to carry out experiments on them. This is achieved by using traps. The most convenient trap is the magneto-optical trap (MOT) which uses a quadrupolar magnetic field in combination with circularly polarized laser beam tuned slightly to the red end of the resonant absorption frequency of atom. With such traps it will be possible to retain atoms and cool them to a temperature below a few hundred micro Kelvin for times long

enough to perform crucial experiments. The background pressure at which the atoms are trapped is low (10^{-8} to 10^{-10} Torr).

In laser cooling and trapping experiments alkali atoms which have a lone electron in the outer most S shell is preferred. They have a electronic ground and excited states which are labelled as $nS_{1/2}$, $nP_{1/2}$ and $nP_{3/2}$. Examples are Sodium, Rubidium and Cesium. Of these atoms Rubidium and Cesium have resonant absorption at 780nm and 852nm respectively between $nS_{1/2}$ and $nP_{3/2}$ levels, while Na has resonant absorption at 589nm. In order to tune at the resonant frequency Na requires an expensive dye laser while Rubidium and Cesium can use simple diode lasers.

2.2. DIODE LASERS

Diode lasers are a very small source of laser light. They are characterized by very high efficiency, a long operating life and cost-efficient production processes. High performance diode lasers therefore have great innovation potential and technical as well as economic advantages. The available wavelength range of diode lasers cover atomic transitions of many inorganic atoms such as Li, Na, Rb, Cs and Ca.

Diode lasers are small devices with dimensions of less than a millimetre. They operate on a wavelength ranging from 0.6 to 1.55 micrometre, depending on the materials of the laser medium. In the diode laser, light is generated in small rectangular active region of typical thickness of 0.1 micron, width 3 micron and length 300 micron, materials of the laser medium.

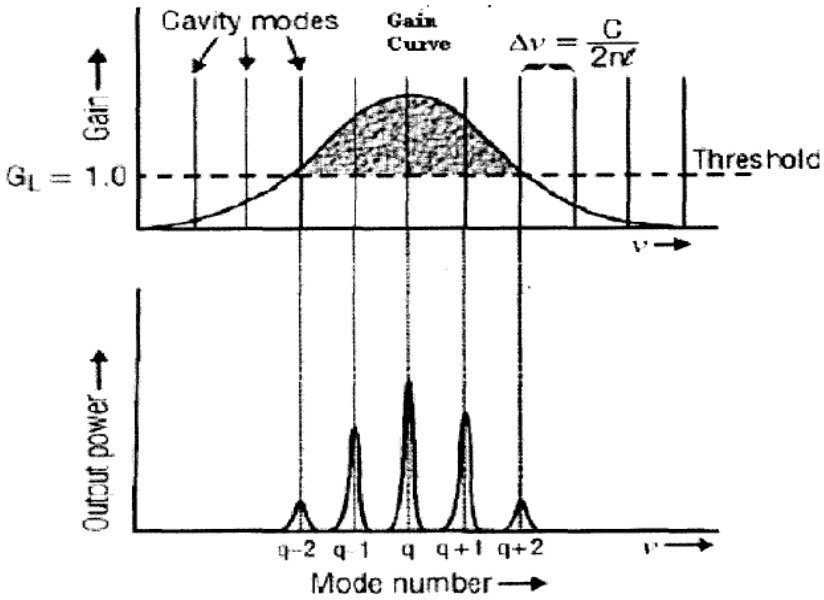

Fig 2.1: Laser modes

The typical output spectrum of a diode laser consists of a series of wavelength peaks corresponding to different longitudinal modes or cavity modes within the structure as shown in Fig 2.1. The spacing of these modes is dependent on the optical cavity length as each one corresponds to an integral number of cavity lengths. The spacing of these modes also depends on the refractive index which in turn is controlled by temperature and carrier density i.e., injection current. The injection current tuning arises because of the heating produced by the current. The injection current also changes the carrier density which changes the index of refraction. Thus there are two tuning parameters - temperature and current, which has to be controlled for stabilizing the Diode laser. In spite of the passive stability of the laser diode injection current and the active stabilization of the temperature, drifts in frequency of few tens of MHz can occur over a period of few minutes. Mechanical vibrations too can cause changes in the laser wavelength. Thus some form of active stabilization of the frequency of the laser is required. This requires a frequency reference, which is obtained by using Doppler free saturated absorption spectroscopy signal of Rubidium atoms.

2.3. EXTERNAL CAVITY DIODE LASER (ECDL)

Laser cooling of atoms demands selective excitation of certain hyperfine transitions, which are separated by a few tens of MHz. This requires lasers with single mode output

and line-width less than the line-width of the transition (few MHz). The laser should be tunable to access any transition of the hyperfine spectrum. The free running Diode laser output is some tens of MHz wide with an output power of 80-150 mW and can be continuously tuned only over certain limited region. The major drawbacks of the free running diode laser, when used for high resolution spectroscopy and laser cooling experiments are multimode spectrum, large line-width, difficulty of continuous tuning, mode hops and stringent requirements on the stability of temperature and injection current. As the laser power increases the spontaneous emission becomes less important at the higher photon densities and hence the line-width decreases.

However the output power of the laser cannot be increased arbitrarily. A more efficient method to reduce the line-width is to make the cavity longer. The external cavity device provides wavelength/frequency tunability also. The extension of the laser cavity length and wavelength selection can be achieved by a wavelength dispersive element as one end of the cavity. Usually diffraction gratings are used. The lasing cavity is now determined by back facet of the diode and the grating as shown in fig.2.2. The increased cavity length L (few cm) reduces intermodal spacing as $\Delta\gamma = \frac{C}{2L}$

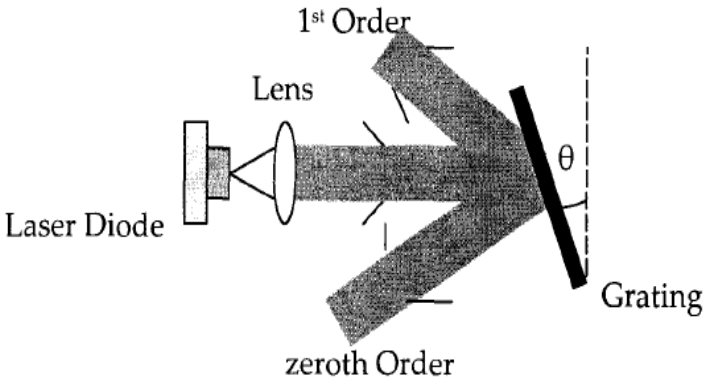

Fig 2.2: Schematic of ECDL

The optical feedback from the grating narrows the line-width of laser output to approximately 1MHz and provides a simple method for tuning the laser over a range of 25nm. The laser has a frequency tuning range of 6nm for a temperature change of 30K. The grating feedback tuning range in the ECDL configuration is much larger than the temperature tuning range. The grating will select the lasing emission from the wide gain spectrum of a free running laser giving a narrow line-width at a desired wavelength. Fur-

thermore wavelength tuning of the output may be achieved by a mechanical rotation of the grating.

The main components of an ECDL are:

- Base Plate: The plate on which all the components are mounted. This is made of material with low thermal coefficient of expansion.

- The Diode Laser: We normally use Sanyo or Sharp diode, which delivers
  80mW power at ~ 100mA current.
  : Wavelength tuning range 775 – 780nm.
- The Collimating Lens: As the output of the laser is divergent, this optical component is most essential. Typically, anti- reflection coated lenses, 4-6 mm focal length are used.
- The Diffraction Grating: We usually use the grating of groove density 1200 lines/mm.

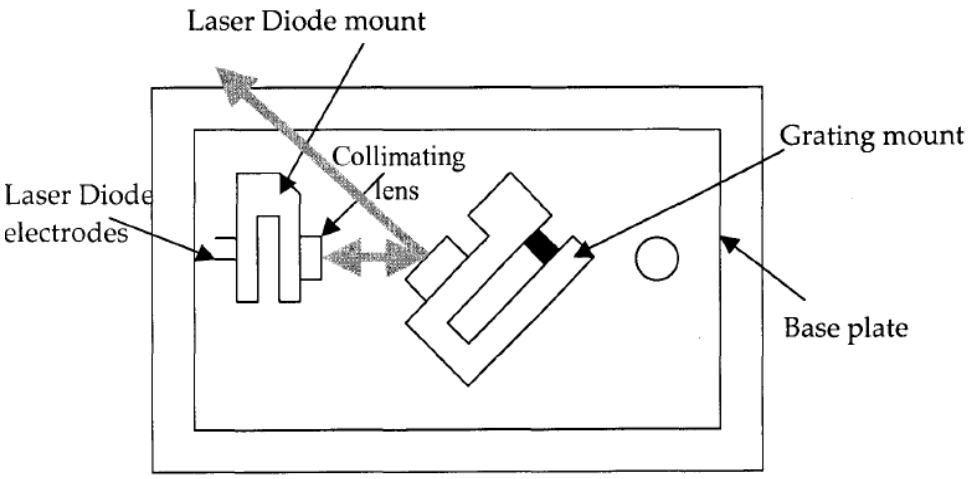

Fig 2.3: Components used in an ECDL

These are arranged as two parts–a package for mounting and collimating the laser diode and another package for mounting diffraction grating along with piezoelectric transducer. These components are mounted on a baseplate. Baseplate, laser-lens mount and grating mount are made up of duraluminium. The enclosure of the ECDL box is made up of aluminium. The threshold current for the mode-hop free operation is 28mA. The maximum power output of this laser diode is 70mw. It can be operated in the tempera-

ture range of -10^0C to $+60^0$C. Its beam divergence angle is 15^0 to 20^0 in perpendicular direction and 6^0 to 10^0 in parallel direction to the junction. The operating voltage of this laser is in between 2V to 2.8V, whereas the operating current has a minimum value of 100mA and has a maximum value of 140mA. The laser diode requires a stable low noise power supply for its operation.

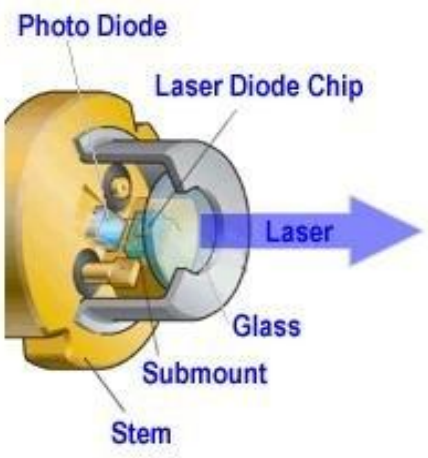

Fig 2.4: Sanyo infrared diode laser

2.3.1. LASER DIODE PROTECTION CIRCUIT

Laser diodes are very sensitive to voltage spikes. The active region is very narrow (1-3micron) and an overvoltage of just a volt will result in extremely large electric fields. The purpose of protection circuit is –

- To protect laser from over voltages or spikes.
- To protect the laser from reverse voltages
- To maintain steady current if there is a momentary reduction in voltage
- To limit the current through the laser diode.

As the pin configuration and the characteristic parameters are different for different laser diodes, separate protection circuits have to be built for each laser diode. Each Laser diode package has three electrodes, one common electrode and two free electrodes, one from laser diode and the other from photo diode. Therefore, according to the electrode configurations the laser diodes can be divided into two major categories, namely "common anode" and "common cathode".

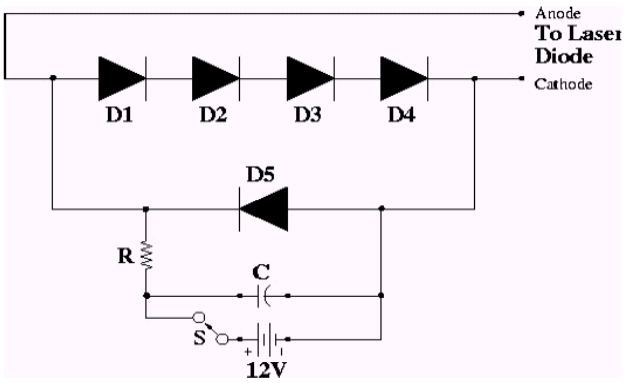

Fig 2.5: Protection circuit for the diode laser

Figure 2.5. shows the protection circuit for the diode laser. The circuit protects the laser diode from any voltage spikes that may come across the laser diode. It consists of four forward biased pn junction diodes (D1 to D5 – 1N4148). These diodes limit the voltage across the laser diode to 2.8V. A reverse biased pn junction diode is included in the circuit to protect the laser diode against reverse voltages.

A capacitor is also included to filter out any spike coming from any source and also prevents a sudden drop in current when the circuit is switched off. The resistor in series with the supply voltage is used as a current limiter.

The series resistance R is calculated as follows:

The operating voltage Vop = 2.8V, Battery voltage VBattery = 12V ……(1)

The operating current Iop = 140mA ……(2)

Therefore laser diode resistance R_D,

$$R_D = Vop / Iop = 20\Omega \quad \text{……(3)}$$

$$Imax = (VBattery / R_L + R_D) < 120mA \quad \text{……(4)}$$

$$(12 / R + 20) < 120mA$$

$$R = 80\Omega \quad \text{……(5)}$$

So the resistance should be 80Ω to get an optimized output from the laser diode.

2.4. TEMPERATURE CONTROLLER

The temperature controller is a vital part of the ECDL setup, since the wavelength of laser light depends on the temperature of the laser mount. It is very essential to control the temperature of the base plate on which the laser diode is mounted.

To achieve this a closed loop system is designed in which a NTC sensor (part of a wheatstone bridge) is placed on the baseplate to sense the temperature of the baseplate, Peltier element is attached to the baseplate to cool or heat the baseplate and an electronic circuit for error signal generation and FET based driver circuitry for the Peltier is implemented. A Peltier cooler, heater, or thermoelectric heat pump is a solid-state active heat pump which transfers heat from one side of the device to the other, with consumption of electrical energy, depending on the direction of the current. The block diagram of the Temperature control unit is shown in figure 2.6 (a).

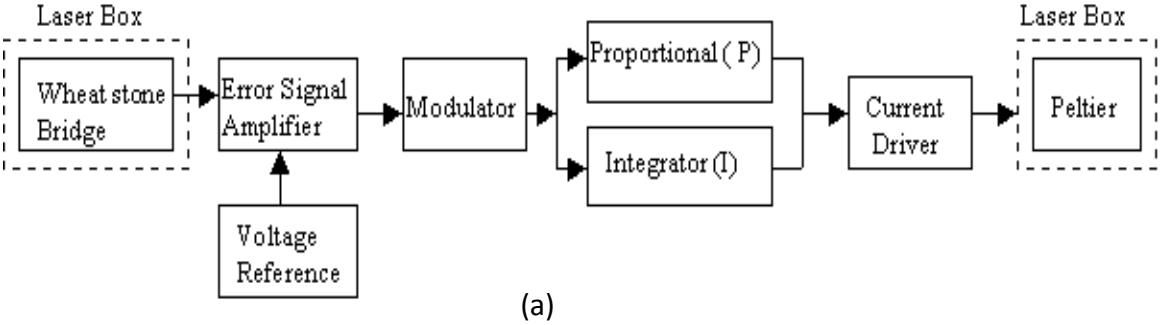

(a)

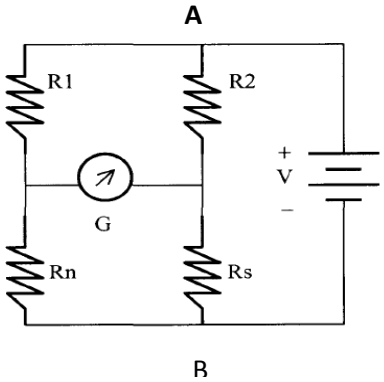

(b)

Fig 2.6 (a) Block diagram of temperature Controller (b) Wheatstone bridge.

The equation for a balanced bridge is given by,

Rn /R1 = Rs /R2 .....(6)

where, Rn is the NTC thermistor resistance, which senses the temperature, Rs is the temperature equivalent resistance, which sets the desired temperature. The temperature of the base plate determines the value of the NTC resistance. A constant voltage source is connected between the nodes A and B. When the actual temperature (sensed by the NTC) T_{AT} of the base plate differs from the set value $T_{ST,}$ the bridge is out of bal-

ance, and an error signal V_{err} appears across the terminal G. The sign of V_{err} depends on whether T_{AT} is more or less than $T_{ST.}$ V_{err} is fed to a Proportional and Integrator (PI) controller stage. The PI applies power

$$W= P (V_{err}) + \alpha\int_t^{t+\tau} V_{err} \quad \text{.....(7)}$$

to the Peltier, where *P* is the proportional gain of the controller,α is the Integration constant. The effect of the integral term is to change the Peltier power, until the time average value of V_{err} becomes zero. We use MOSFETs 2SK1058 (PMOS) AND 2SJ162 (NMOS) as current drivers for driving the Peltier. The PI controller decides the direction and the amount of current to be sent to the Peltier to achieve the required cooling or heating of the baseplate. Initially only the proportional stage is switched on, and current is sent to the Peltier and base plate starts cooling down and then the integrator stage is switched on, which integrates V_{err} over a certain time. The integrator stage ensures that V_{err} reaches zero rapidly, and therefore T_{AT} becomes equal to $T_{ST.}$ The temperature controller stabilises the laser temperature to about $\pm$ 10 mK of its set value within 20 minutes.

2.5. SATURATION ABSORPTION SPECTROSCOPY

The simplest spectroscopy that can be performed with the laser diode is to observe the absorption and Doppler-free saturated absorption of Rubidium atom. This can be easily done in a small glass Rubidium vapour cells in which atoms are at room temperature. It also provides the simplest way to determine the short and long term frequency stability and tuning behaviour of the laser frequency.

Saturated absorption spectroscopy is a kind of nonlinear spectroscopy. In the linear spectroscopy a single propagating wave is incident on the sample, some photons are absorbed and only some fraction of the wave reaches the detector. Here the radiation reaching the detector is proportional to the radiation incident on the sample. In nonlinear spectroscopy there are two counter propagating beams which interact with the same atoms in the region where they intersect. In this case the radiation reaching the detector is dependent on both the beams. Saturated absorption eliminates Doppler broadening to uncover hyper fine structure. Rubidium sample can be theoretically

treated as hydrogen like atom because of its single valence electron. Rubidium can absorb radiation when the laser frequency corresponds to a difference in energy levels, exciting the valence electrons to a higher state. The absorption spectra in traditional spectroscopy are characterized by broad signals around each absorbed frequency. This is a result of Doppler effect. Doppler free saturated absorption spectroscopy is insensitive to this effect and thus allows the splitting between energy levels of a sample to be measured with much greater precision. When the laser is tuned to resonant frequency Doppler free saturation absorption spectroscopy arises because the pump beam saturates the transition, resulting in non-absorption of the probe beam.

2.5.1. EXPERIMENTAL SET-UP

The experimental set up for the saturation absorption spectroscopy is shown in the fig 2.7. In a MOT setup there will be two lasers namely Cooling Laser and the Repumper Laser. Rubidium (Rb) atoms have 4 hyperfine transitions, two for ^{85} Rb isotope and two for^{87} Rb isotope. It is essential to lock the cooling and repumper lasers to one of these transitions. This is achieved with a Saturation absorption setup which has an optical setup, which includes mirrors, beam splitters and Rubidium vapour cell and a Photo Detector Circuit**.**

Saturation absorption setup includes Vapour cell, glass plates and beam splitters. The optics is arranged such that incoming laser light is split into two weak beams (called as Reference and Probe beams), which pass through the vapour cell, and a strong Pump beams which counter propagates through the same cell. Pump and probe beams are made to coincide within the vapour cell. The two beams Reference and Probe (with Pump overlapped) are made to fall on two identical Photo detectors. When the line width of the laser light is ~ few hundreds of MHz and frequency is in resonance with certain hyperfine transition, the difference of the outputs of Photo detectors will result in the Doppler free hyperfine transition line which can be used as a reference frequency of the laser diode.

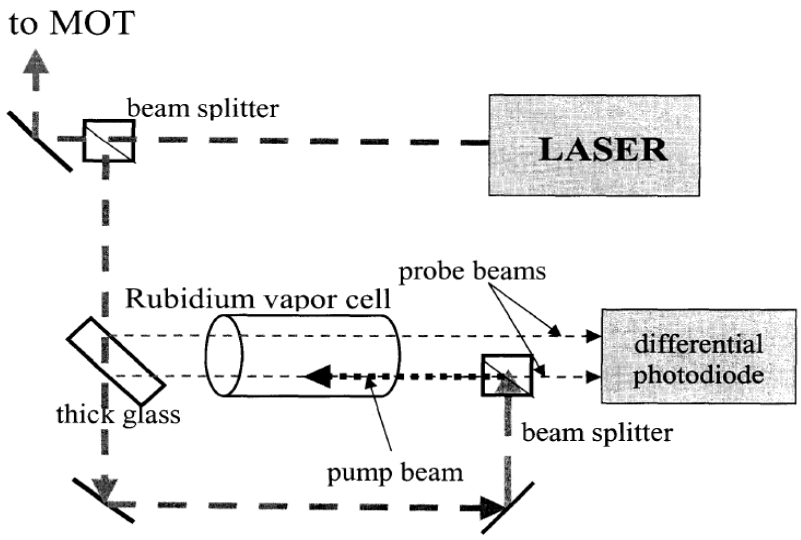

Fig2.7: Experimental set up of saturation absorption spectroscopy

The signals that are desired to be displayed on the Oscilloscope are Doppler broadened signal of the unsaturated probe, saturation absorption signal of Rb85 (the difference signal) along with the ramp signal. The laser can be locked at a particular frequency by monitoring these signals.

2.6. FREQUENCY LOCKING

The frequency of the diode laser can be locked to the saturated absorption component with the help of an electronic servo control, where any deviation from the locked frequency is taken as the error signal and applied to the external cavity component for controlling the cavity length, so as to pull the laser frequency to the locked position. One method of locking the laser frequency is through Lock-in amplifier. In this technique, the PZT in ECDL is modulated sinusoidally at a reference frequency (800Hz) and the resulting modulated saturation absorption signal is phase sensitively detected at the reference frequency and the laser frequency is locked at the peak. Any deviation from the locked position again generates an error signal which after smoothening and amplification is applied to PZT.

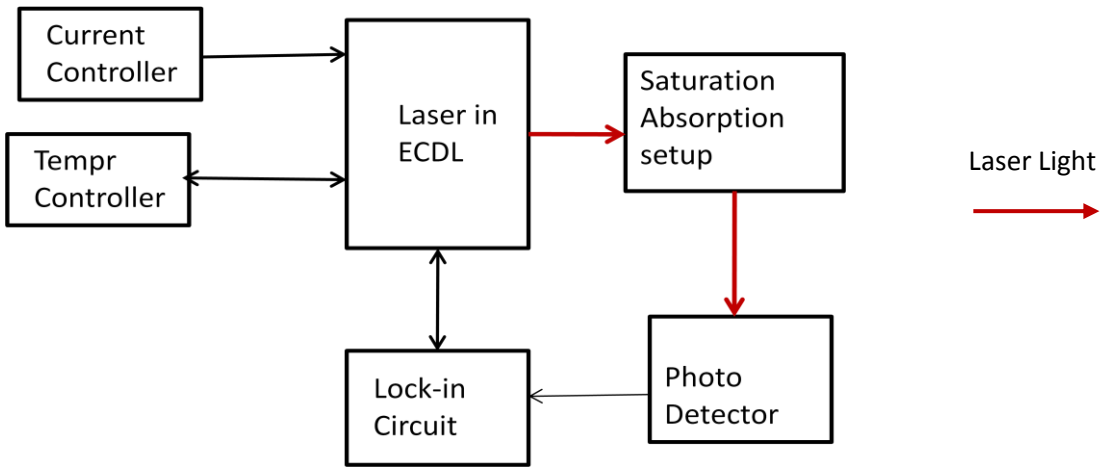

Fig 2.8: ECDL setup for Frequency Locking of the Laser

The laser is scanned across the hyperfine lines by sending a ramp signal to the piezo-electric transducer (PZT) attached to the grating mount. Lock-in circuit produces the ramp signal, which is sent to PZT in ECDL. We then reduce the ramp amplitude so that the frequency scanning gives rise to only one of the peaks of the saturated absorption spectrum, the one at which we want to lock the laser frequency. As the ramp signal sent to the PZT is modulated using sine wave, the detector output, which earlier gave smooth peak, is now distorted due to modulation. This new signal is multiplied in a multiplier stage in the lock-in circuit with the same sine wave which was used to modulate the ramp signal. The output of this stage is passed through a low pass filter.

A dc signal is obtained which is derivative corresponding to the peak of the hyperfine absorption where we want to lock the frequency. The error signal produced (it is the de-rivative of the actual signal) crosses zero exactly at the position of the peak of the spec-trum, where the laser should be locked, and is positive at one side and negative at the other side. This is a feedback signal to lock the frequency of the laser exactly at the top of the peak in the spectrum. The error signal monitoring thus becomes an excellent indi-cator of the magnitude and spectral characteristics of the compensated noise.

Chapter 3: AOM locking

3.1. Introduction

Precision experiments like the laser cooling of neutral atoms to few hundred micro-kelvin ranges in temperature requires the source laser's frequency to be maintained within a few MHz. To control the laser frequency, various techniques including measurement of beat frequency [1], servo based feed-back method [2] and optical feedback [3] have been tried. Commercial lasers used in these experiments employ sophisticated feedback mechanism to maintain the laser frequency to the desired accuracy. However, in many applications the original laser frequency (at 10^{14} Hz) has to be shifted by a few hundred MHz using AOMs. The output RF frequency of an AOM, drifts from its initial set value due to AOM crystal getting heated up, and due to fluctuations in the driving voltages. The drifts from the set value vary over a range of 0.4 MHz to 0.9 MHz. We have developed a feedback mechanism to control such changes in the frequency of the RF output produced by the AOM driver. We correct for the frequency change by changing the AOM tuning voltage. To this end, we have developed a PI based feedback mechanism which works in such a way that any error produced due to the shift in the RF output is detected and relevant control action is taken by sending a feedback signal.

3.2. Principle of operation of AOM

An acousto-optic modulator (AOM) also called a Bragg cell, uses the acousto-optic effect to diffract and shift the frequency of light using sound waves (usually at radio-frequency). They are used in lasers for Q-switching, telecommunications for signal modulation, and in spectroscopy for frequency control. A piezoelectric transducer is attached to a material such as glass. An oscillating electric signal drives the transducer to vibrate, which creates sound waves in the glass. These can be thought of as moving periodic planes of expansion and compression that change the index of refraction. Incoming light scatters off the resulting periodic index modulation and interference occurs.

3.3. System Design

The block diagram is represented in the form of the basic block diagram of a closed loop system. Figure 3.1 gives this basic block diagram of the circuit we designed and constructed to implement the feedback control scheme. The Plant in our setup is the AOM, whose output frequency is the important parameter here which we want to control and stabilize. ”Measuring Device” is the block which measures the RF signal we are interested, and gives a DC voltage output proportional to it. Controller in this setup is a PI based controller which generates an error signal, which is fed back to the plant for precise control.

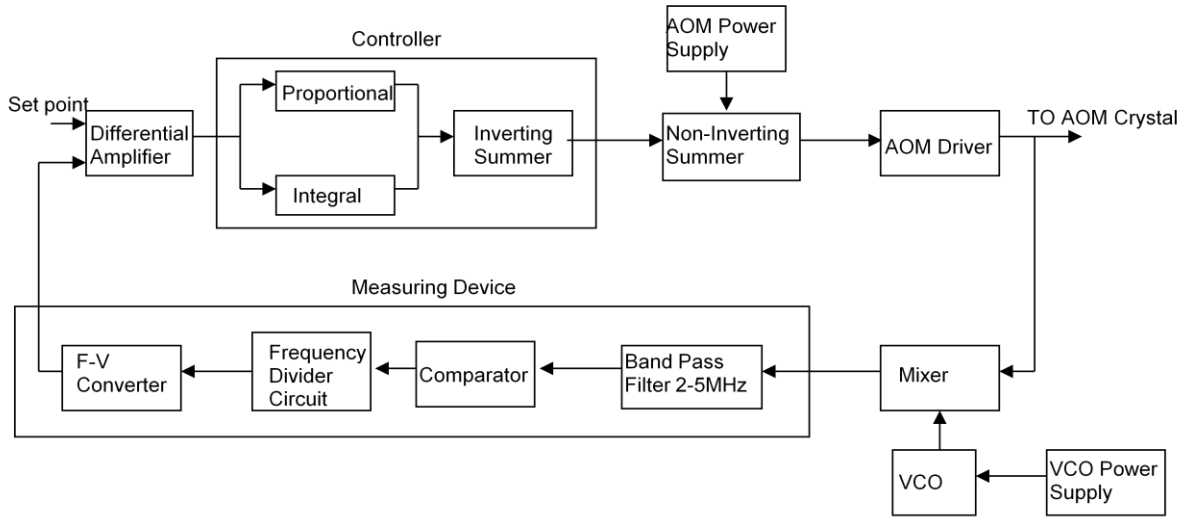

Fig3.1. Basic block diagram of the setup

3.3.1. Plant

In our case, the Plant unit is the AOM driver and AOM power supply with a Non Inverting summer. The corrective signal out of the PI controller and the tuning voltage from the AOM power supply are fed as inputs to the non inverting summer and the output is then fed as the corrected tuning voltage to the AOM driver. The AOM driver produces a RF signal output proportional to the tuning voltage fed to it. Any fluctuations arising internally inside the RF Driver which affects the RF frequency output of the AOM will be corrected by the PI controller of the feedback system. The PI controller works in such a fashion, that the net voltage going into the AOM driver is a constant tuning voltage and hence the RF output remains constant.

3.3.2. Proportional-Integral Controller

The basic layout for a PI controller used in our circuit is shown below in figure 3.2. Error signal is fed both to the P and I blocks and their outputs are summed using an inverting amplifier. The proportional controller mechanism acts on the value of the error and gives an output which is proportional to the error by multiplying the error by the controller gain. This voltage is applied to the controller's output almost immediately, mainly limited only by the signal transit time.

The integral term integrates the error over a controllable duration and applies the result to the controller output thereby eliminating the controller offset error. Basically what it does is that it increases the type number of the open loop systems by one and therefore, if the steady state error of the system is constant, it removes it totally. The residual error which remains after a proportional stage is eliminated by using the integrator.

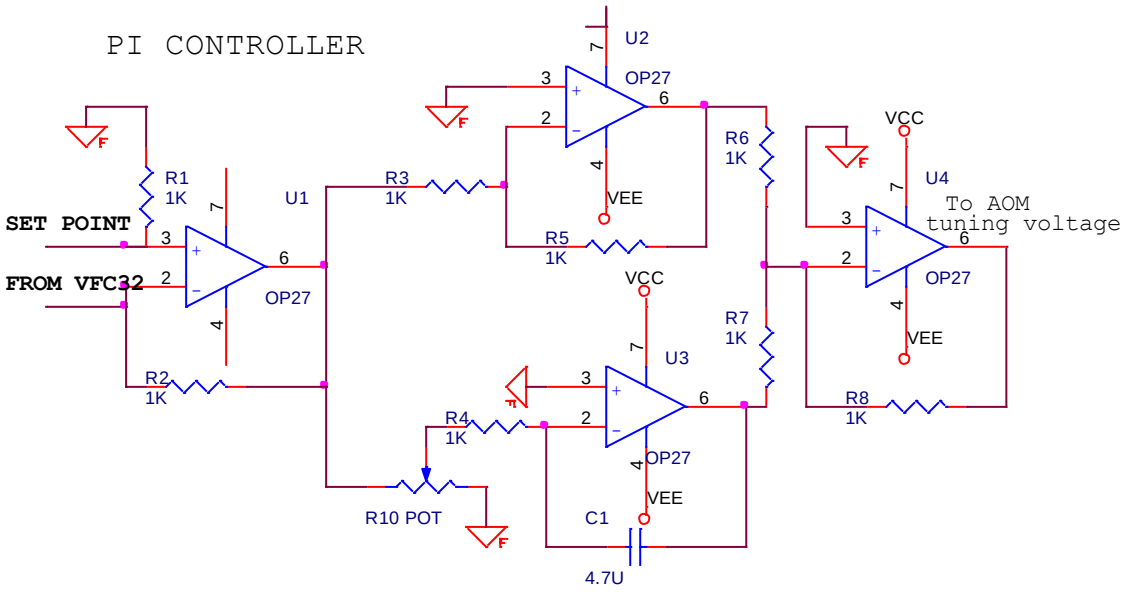

Fig 3.2. PI controller circuit diagram.

3.4. Measuring Device

In our setup Measuring Device block includes Band-pass filter, Comparator Circuit, Frequency Divider circuit and Frequency to Voltage (FVC) Converter. Designing and construction of the measuring device of the system is the most important part of the setup. It involved measuring the RF signal as precisely as possible because the accuracy of this would decide the accuracy of the whole system. Measuring the output frequency is a

difficult task as it becomes difficult to isolate the signal that we require. To achieve this we first mix the RF output signal of the AOM with the output of a Voltage controlled Oscillator (VCO) using a Mixer [5]. In our circuit we use ZOS-150 VCO and ZLW-1, level 7 Mixer from Minicircuits. The inherent fluctuations of VCO are measured to be about 0.1 MHz (S.D: 0.02809). After the mixer stage, we pass it through a Band pass filter.

The output of the VCO is tuned to a frequency value such that the difference between VCO frequency and the RF output signal frequency of the AOM is within the range of band pass filter. For the Band pass filter design we have used Sallen Key Topology [6]. The design formulas for the Low Pass Filter and High Pass Filter of figure 3 are denoted as R13,R14 (HPF) and R16, R15 (LPF) = $1/2\sqrt{2}\pi C\,Freq$.----------(1)

3.4.1. Wide Band Pass Filters

This is done by cascading a HPF (for low end frequency of the filter) with a LPF (for high frequency end of the filter). The high pass filter comes first, followed by the LPF such that the overlap region is the desired pass band frequency range. When designing band-pass filters, the parameters of interest are the gain at mid frequency (Am) and the quality factor (Q), which represents the selectivity of a band-pass filter. The frequency drifts we have observed in few models of AOM vary from 0.4MHz to 0.9MHz. Based on these values, we have designed the system to control the drifts upto +/- 1.5 MHz, making provision for any spurious drifts. The range of corrections is decided by the bandwidth of the BPF.

+/- 1.5MHz window gives a stability of one part in 10 million in the laser frequency. A band pass filter was designed for a range of 2-5 MHz using AD847, which is a very high speed operational amplifier with a very high slew rate of 300V per micro second and high gain bandwidth product of 50 MHz which makes it ideal for the kind of application that we require. Different values of capacitors and resistors used in the circuit were calculated from formula(1).

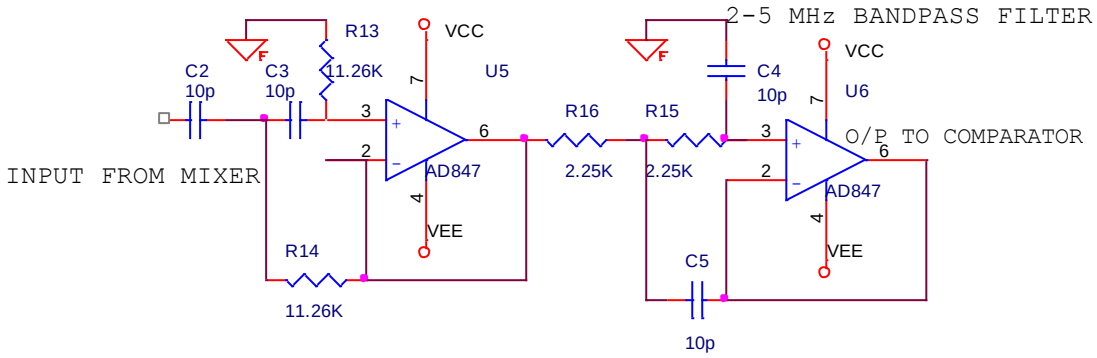

Fig.3.3 Filter circuit

3.4.2. Voltage Comparator Circuit

After passing through the band pass filter we need to convert this signal to a corresponding value in voltage. For this purpose a frequency to voltage converter is designed. Various stages of this converter are explained below. The beat signal coming from the filter, which is a sine wave, is converted to a square wave using a high speed comparator LM 360. The LM360 is a very high speed differential input, complementary TTL output voltage comparator, with improved characteristic over the µA760/µA760C. The device has been optimized for greater speed, input impedance and fan-out, and lower input offset voltage.

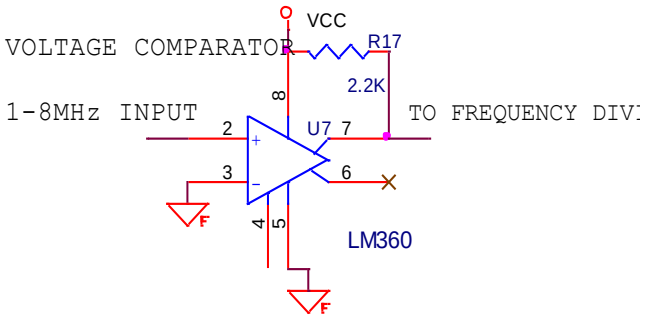

Fig 3.4 Voltage Comparator

3.4.3. Divide-by-16 Network

The comparator circuit is followed by divide-by-16 circuit (figure 3.5) which is constructed by connecting in series two divide by eight networks. This is done using DM 7490 IC which is a decade and binary counter.

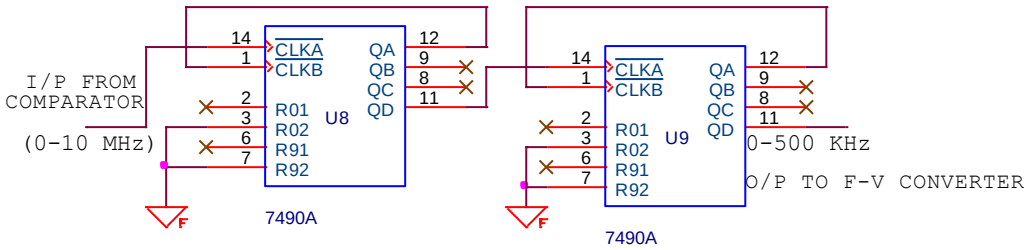

DIVIDE BY 16 NETWORK

Fig 3.5 Divide-by-16 network using two DM 7490

3.4.4. Voltage-Frequency Converter (VFC 32)

The output of the divide-by-16 network is passed through Frequency to Voltage converter circuit (figure 3.6). VFC32 is used for Voltage to Frequency and Frequency to Voltage conversion. The functioning of VFC 32 [7] is as follows. The VFC32 voltage-to-frequency converters provide an output frequency accurately proportional to its input voltage. As the output is digital open-collector, it is compatible with all the common logic families. It's integrating input characteristics gives the VFC32 excellent noise immunity and low nonlinearity. By tuning external capacitor and resistor, Full-scale output frequency can be achieved over a wide range.

VFC 32 [7] works on the principle of charge balance. The input signal current which is equal to Vin/Rin is first integrated by the Integrator, Cin producing a downward output voltage. VFC32 has inbuilt integrator, 1 ma reference current source and one-shot multivibrator. When the integrator output ramps to the threshold voltage of the comparator, one shot is triggered on, and 1ma reference current is connected to the integrator input for the one-shot period, and now integrator generates output upward ramp. After the one-shot period is over, integrator starts to ramp down. This oscillation between upward ramp and downward ramp causes balance of charge between input signal current and the reference current.

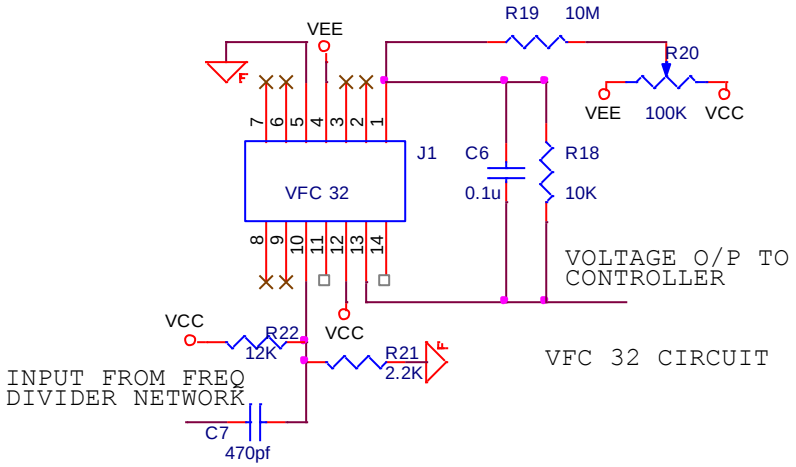

Fig 3.6. VFC 32 Circuit configured as Frequency to Voltage Converter

A graph representing the linearity of the measuring device block which includes Band pass filter, Comparator, Frequency Divider Circuit and F-V converter over an entire frequency range of 1-8 MHz is shown in Figure. 3.7.

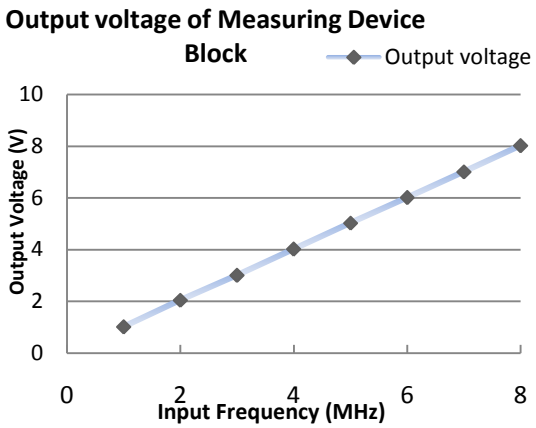

Fig 3.7. Linearity curve of Measuring Device Block from 1MHz to 8MHz

3.5. Principle of Operation

When the output frequency of the AOM drifts from the desired set value due to internal changes, the closed loop system will work to bring the system back to its desired state. To understand this, let us analyze a case in which RF signal produced by an AOM for a tuning voltage of say 5V, is 72.22 MHz (a standard value). Due to some internal changes, this RF signal frequency increases to say 72.32 MHz. Now the system should work in such a way to change the output back to its initial desired state.

This is done as follows. The RF output signal from the AOM (72.32MHz) is mixed with VCO output which is fixed at 69.32 MHz. This frequency is chosen such that the differ-

ence frequency falls within the range of the Band-pass filter (2 – 5 MHz). For this example, the difference beat frequency is 3.0 MHz which is then fed into the Mixer. The Mixer output has f1, f2, f1+f2, f1-f2 (beat frequency) and also harmonics. The Band pass filter we have designed has a range of 2 to 5 MHz, which allows only the difference signal to proceed further in the system. This signal has to be expressed in terms of voltage for further analysis.

VFC32 takes only square wave input in the range of 0.1 to 1 MHz. LM 360 is a high speed comparator, which converts the sine wave at the Band-pass filter output to square wave. This is followed by a Frequency divider circuit which is designed to convert a signal in the range of 0 to 10 MHz to 0 to 500 KHz. This is fed to the frequency to voltage converter, which gives a corresponding output voltage. The complete setup is scaled in such a way that an input of 3 MHz produces an output voltage of 3V. This is one of the inputs to the Differential amplifier. The other input is the set point (value that corresponds to the required output i.e. 2.9V). This value corresponds to 72.22 MHz - 69.32 MHz = 2.9 MHz which corresponds to 2.9V.

The two inputs (Set point and Output from VFC) are given to a differential amplifier and the error voltage is obtained and then fed to the PI controller. The output of the controller which is -0.1V, together with the AOM supply voltage of 5V produces an output signal of 4.9V. This acts on the AOM driver to produce a shift of 72 MHz. The frequency shift that has occurred due to the previous internal change together with the 72 MHz signal, produce a desired signal frequency of 72.22 MHz, thereby reverting the system back to the desired set value.

3.6. Results

The experimental setup which includes AOM, AOM Driver and control electronics unit which includes Mixer, Measuring device, Differential summer and Controller is assembled and we tested the system for various AOM frequency settings. We tested the system by observing and tabulating the voltage outputs at Set point, VCO tuning voltage, FVC output and final output voltage which is the AOM tuning voltage and importantly AOM output frequency (Fig. 3.8) for different settings over several hours. The set point

is one of the inputs and FVC output is the other input to the differential amplifier. The set point is set to the value as per the requirements of experiment. Figures 3.9 and 3.10 shows the measurement of the FVC output and Final output which is fed to the AOM as tuning voltage for two different frequency outputs. We see that the feedback control is very effective and the frequency of the AOM is maintained at the desired set value. +/- 1.5MHz window gives a stability of one part in 10 million in the laser frequency.

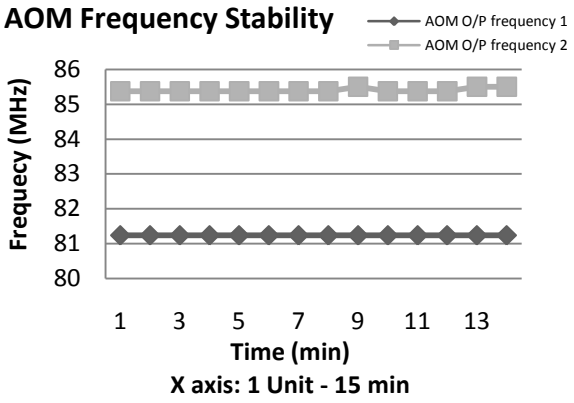

Fig 3.8.: Measurement of AOM output frequency at two different frequency outputs.

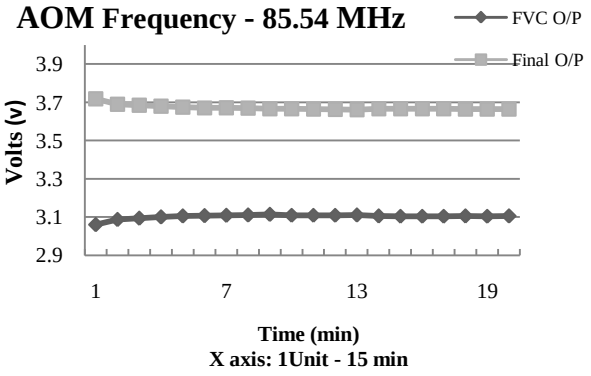

Fig 3.9. Measurement of FVC output and final output which is fed as tuning voltage to the AOM driver with set-point different from the AOM tuning voltage.

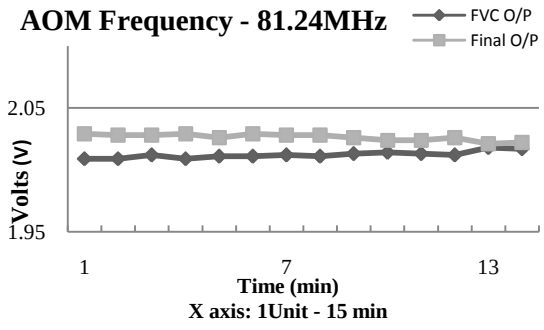

Fig 3.10. Measurement of FVC output and final output which is fed as tuning voltage to the AOM driver with set-point close to the AOM tuning voltage.

3.7. Conclusion and Publications:

We have presented a simple and cost effective feedback mechanism to control inherent changes in the AOM driver. This mechanism stabilizes the absolute frequency output of the AOM with an accuracy upto few KHz. This method will be useful in situations where the AOM driver voltage is not very stable and faster and stable control of the output frequency is desired.

This work was presented as a paper titled

"Feedback control Mechanism for Acousto-Optic Modulator",

M S Meena , V Arun , SahilSanan and Andal Narayanan

has been published in Instrumentation Society of India (ISOI), IISC, Bangalore in December 2010 issue. **(JL. of Instrumentation Soc. Of India**, Vol. 40 No. 4 , December 2010).

3.8. Quantum Walk experiments:

Quantum walk experimental setup mainly includes an AOM Driver and four AOM crystals for shifting the frequency of the light. For getting the interference fringes it is essential excite all AOM crystals with RF signals in phase. Two AOM crystals are driven from a single RF amplifier (ZHL-1-2W). To achieve this, a setup is designed using RF amplifier (ZHL-1-2W Mini-circuits) and attenuators to achieve the desired power outputs, phase matching and identical path lengths (figure 3.11).

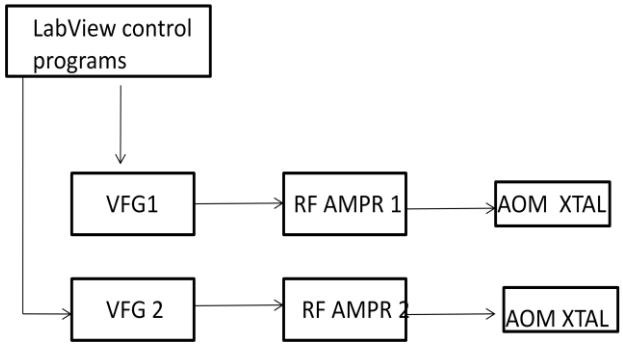

Fig 3.11. Block diagram setup for Quantum walk experiments

To study the quantum walk of light in frequency space, it was required to introduce phase noise in the Versatile Function generators (VFG), which we achieved using Lab-VIEW programs, which enabled us to introduce systematic phase noise between signal generators which were used to drive the AOMs.

This work resulted in interesting results which was published in **Physical Review A, Phys.** Rev. A 84, 042322 (2011) titled

"Quantum walk of light in frequency space and its controlled dephasing" , Deepak Pandey, Nandan Sathpathy, Meena M.S. and HemaRamachandran.

4. Magneto Optic Trap (MOT) Experiments

4.1. Experimental Ideas and details:

In laser cooling experiments to trap the atoms in a Magneto Optical trap, a pair of Anti-Helmholtz magnetic coil is used to produce a magnetic field around the UHV chamber which is evacuated upto pressures of 10^{-10} mbar. The anti-Helmholtz coils for the magnetic trapping are connected in series to ensure that the current flowing through each coil is equal in magnitude, though opposite in direction.

3 pairs of counter propagating laser beams are fired from +/- x,+/- y and +/- z directions to reduce the average velocity of the atoms to about 10cms^{-1} (~100µK), from ~300 ms^{-1} at room temperature. At the point of intersection of zero crossing of the magnetic field and 3 laser beams, we achieve the cold and trapped cloud.

To capture the atoms, the magnetic field needs to be switched on. For characterising the MOT, i.e. to calculate number of atoms, decay rate etc, it is essential to switch off the MOT. Most of the measurements are made after the magnetic field is switched off, i.e. during the decay time. In this regard we need a Switching Circuit which switches the magnetic coils on and off at currents up to 5A, up to 100 Hz. We have designed an IGBT based switching circuit.

4.2 Magnetic coils switching circuit:

4.2.1. IGBT Mitsubishi CM–200DU-12F[8].

Structure and operation of IGBT module

The IGBT, Insulated Gate Bipolar Transistor, is a switching transistor that is controlled by voltage applied to the gate terminal. Device operation and structure are similar to those of an Insulated Gate Field Effect Transistor, more commonly known as a MOSFET. The principal difference between the two device types is that the IGBT uses conductivity modulation to reduce on-state conduction losses.

The npn BJT is a three junction device that requires a continuous current flowing into the base region to supply enough charges to allow the junctions to conduct current. Because the MOSFET and the IGBT are voltage-controlled devices, they only require voltage on the gate to maintain conduction through the device. The IGBT has one junction more than the MOSFET, and this junction allows higher blocking voltage and conductivity modulation during conduction. This additional junction in the IGBT does limit switching frequency [9].

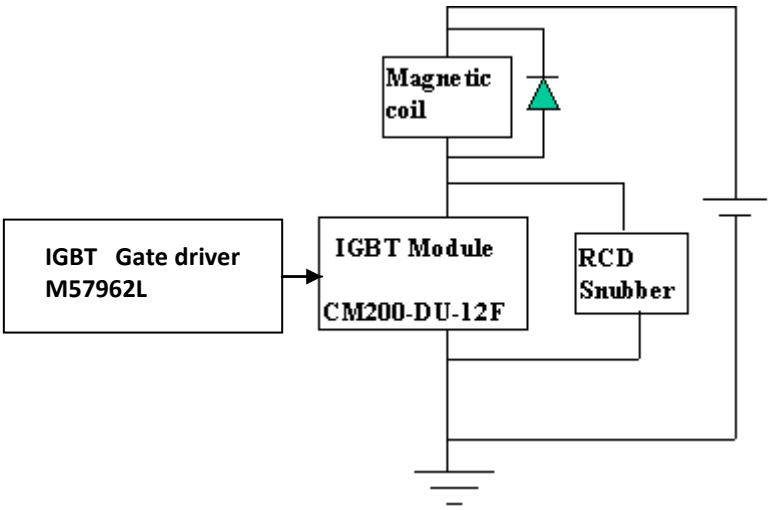

Fig 4.1. IGBT switching circuit

IGBT CM-200DU-12F:

Mitsubishi IGBT modules are designed to be rugged, low loss and easy to use. They give low on-state saturation voltages while maintaining the high switching speed needed for 20 KHz operation. Each module consists of two IGBT's in a half bridge configuration with each transistor having a reverse-connected super-fast recovery free wheel diode.

Specifications: Ic – 200A, Vces-600v, Dual IGBT module and 250v Trench Gate

4.2.2. M57962L IGBT driver:

This is a Hybrid Gate Driver from Mitsubishi designed to convert logic level control signals (0 to 5V) into optimal IGBT gate driver (-12v to +15v) fig 4.2. Input signals are isolated from the IGBT drive using high speed optocouplers with 15,000 V/ms common mode noise immunity. Mitsubishi IGBT drivers are designed to provide the pulse cur-

rents necessary for high performance switching applications and to maintain sufficient off bias to guarantee ruggedness. They also provide short-circuit protection.

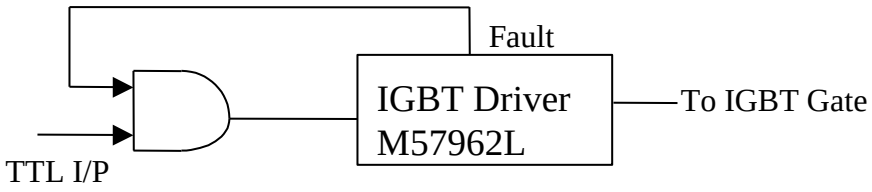

Fig 4.2 IGBT Driver circuitry

Depending on the gate input (fig 4.2), when the gate is at +15v, IGBT is switched on and current flows through the Magnetic coil and IGBT. When gate is at –12v, IGBT is switched off. Also a clamp diode which is a fast recovery diode is connected across the coil, to maintain current flow in the magnetic coils when IGBT is switched off.

4.2.3. Snubber Circuit:

(i). Turn-off Surge Voltage

Turn-off surge voltage is the transient voltage that occurs when the current through the IGBT is interrupted at turn-off. A voltage (VS) equal to Lb x di/dt appears across Lb (Bus Inductance) in opposition to increasing current in the bus. The polarity of this voltage is such that it adds to the DC bus voltage and appears across the IGBT as a surge voltage. In extreme cases, the surge voltage can exceed the IGBT's VCES rating and cause it to fail. In a real application the parasitic inductance (Ls) is distributed throughout the power circuit but the effect is the same[9].

(ii). Free-Wheel Diode Recovery Surge

A surge voltage similar to the turn-off surge can occur when the free-wheel diode recovers. The parasitic bus inductance (Lb) develops a surge voltage equal to Lb x di/dt in opposition to the decreasing current. In this case, the di/dt is related to the recovery characteristic of the free-wheel diode. Some fast recovery diodes can develop extremely high recovery di/dt when they are hard recovered by the rapid turn on of the lower IGBT. This condition referred to as "snappy" recovery, can cause very high transient voltages.

Snubber circuits are usually used to control turn-off and free-wheel diode recovery surge voltages. In some applications snubber circuits are used to reduce switching losses in the power device. In our setup we use a RCD snubber across IGBTs.

4.2.4. Hardware Details:

Driver PCB: In our setup we have two GBTs, and hence two IGBT drivers are required. A PCB was designed so that IGBT drivers can be mounted in a single PCB. Layouts were made in Orcad software, PCB was assembled and tested for the specifications.

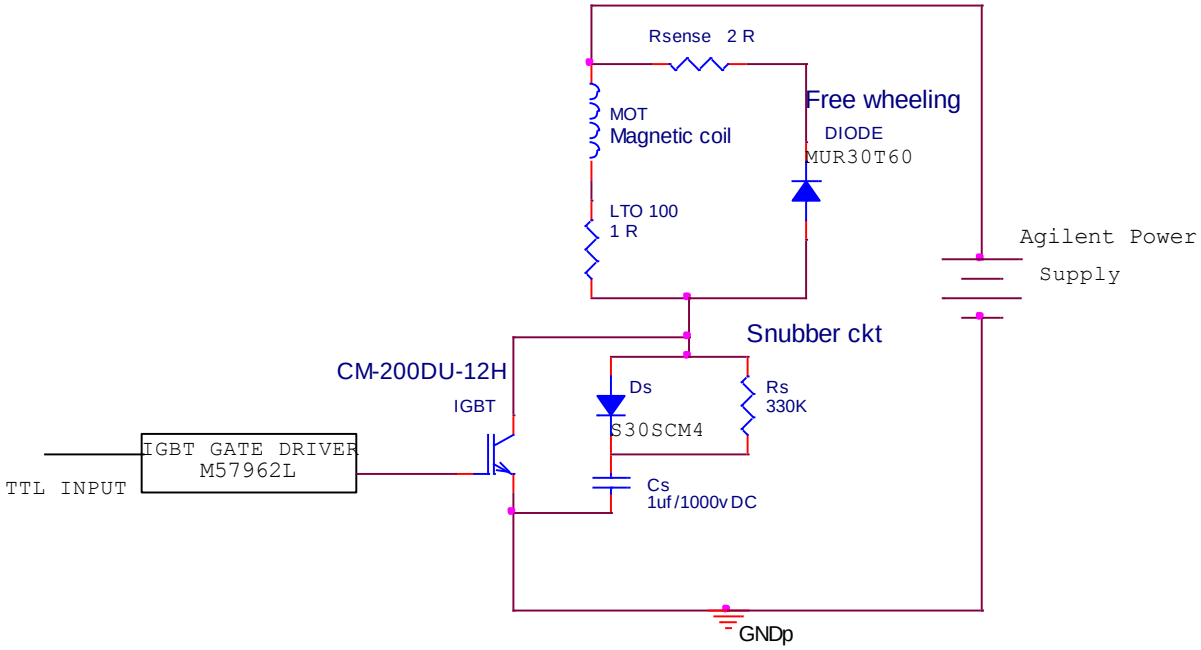

(a)IGBT Main Switching Circuit

(b) IGBT Driver circuit

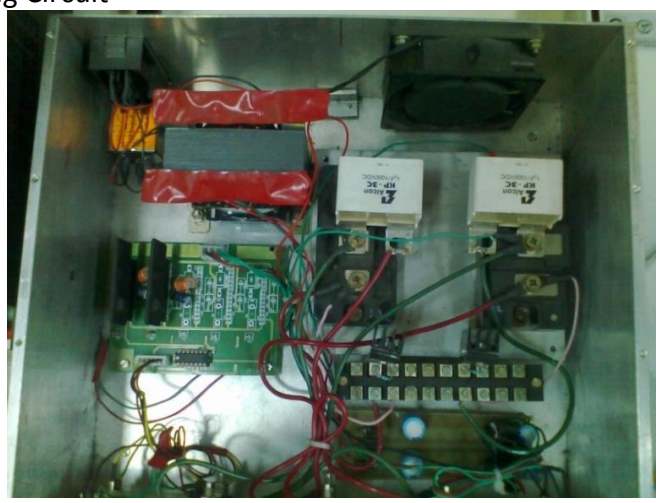

(c) Complete Assembly unit

Fig 4.3 : Magnetic coils switching circuits

.

4.2.5. Back EMF:

Each Magnetic coil consists of 26 layers, 26 turns in each layer, which is wound using 1.6 mm enamelled copper wire, diameter of the coils is 26 cms, with total resistance of 5 ohms and total inductance of about 50 mH. In a magnetic coil every current winding behaves as an inductor. The following formulae explains the relationship between back EMF (e), inductance (L), current (I), stored inductive energy (E) and the resistance (R)

$e=-L\, di/dt$ ---- (1)

$E=1/2\ LI^2$ ----(2)

$I=I_0 exp^{[-t(L/R)]}$ ---(3)

In switching circuits used for driving inductive loads it is essential to have a protection circuit to avoid damages to output transistor or integrated circuits from back EMF voltages.

4.2.6. Types of Transient Suppression:

The basic techniques for suppression of transient voltages from magnetic coils are explained below. The suppression device may be in parallel with the coil or in parallel with the switch used to control the coil. It is normally preferred to have the suppression parallel to the coil since it can be located closer to the coil. When the suppression is in parallel with the coil, any of the following may be used.

a. A bilateral transient suppressor diode that is similar in V-I characteristics to two zener diodes connected cathode to cathode (or anode to anode).
b. A reverse-biased rectifier diode in series with a zener diode such that their anodes (or cathodes) are common and the rectifier prevents normal current flow.
c. A metal-oxide-varistor (MOV).
d. A reversed-biased rectifier diode in series with a resistor.
e. A resistor, when conditions permit its use, is often the most economical suppression.
f. A reversed-biased rectifier diode.

In our circuit we have used reverse biased fast switching diode (MUR3060T) in series with a low resistance, low inductance thick film resistor LTO 100 (1ohm)) across the magnetic coil for the suppression of back emf. We have connected MUR3060T diode as freewheeling diode which is 30A Fast recovery rectifier, with Peak Reverse Voltage up to 600V.

4.2.7. Current modulation using IC XR2206:

In the experimental setup to achieve the required results the entire experiment needs to be automated. Each experiment has a particular sequence in which devices like shutters, AOMs etc has to be switched on/off and Magnetic coil currents has to be varied. The currents in magnetic coils need to be ramped up and down in time intervals of few milli-seconds.

Initially for testing modulation of Magnetic coil currents, the scheme which we followed is as follows:

1. Give the TTL trigger signal to the switching circuit (as shown in figure 4.1)
2. For current modulation, according to the output current required, give a corresponding analog ramp signal to the current programming inputs of programmable power supply.

To achieve this we have designed a circuit using IC XR-2207 which is a monolithic voltage-controlled oscillator (VCO) integrated circuit featuring excellent frequency stability and a wide tuning range. The circuit provides simultaneous triangle and square wave outputs over a frequency range of 0.01Hz to 1MHz. It is ideally suited for FM, FSK, and sweep or tone generation, as well as for phase-locked loop applications.

The XR-2207 has a typical drift specification of 20ppm/°C. The oscillator frequency can be linearly swept over a 1000:1 range with an external control voltage; and the duty cycle of both the triangle and the square wave outputs can be varied from 0.1% to 99.9% to generate stable pulse and saw tooth waveforms.

This IC XR2207 has two outputs (a) TWO - Triangle Wave output – which is fed to the current programming pins of power supply (b) SWO - Sync Output- which is in sync with the triangle wave output and it is fed to the switching circuit. A Ramp and sync generator circuit is designed using IC XR2207, tuning resistors and capacitors to generate ramp signal of frequency 10 Hz. The amplitude of this ramp signal can be varied, for programming the current output of the power supply.

The circuit diagram for the test setup is as shown in figure 4.4.

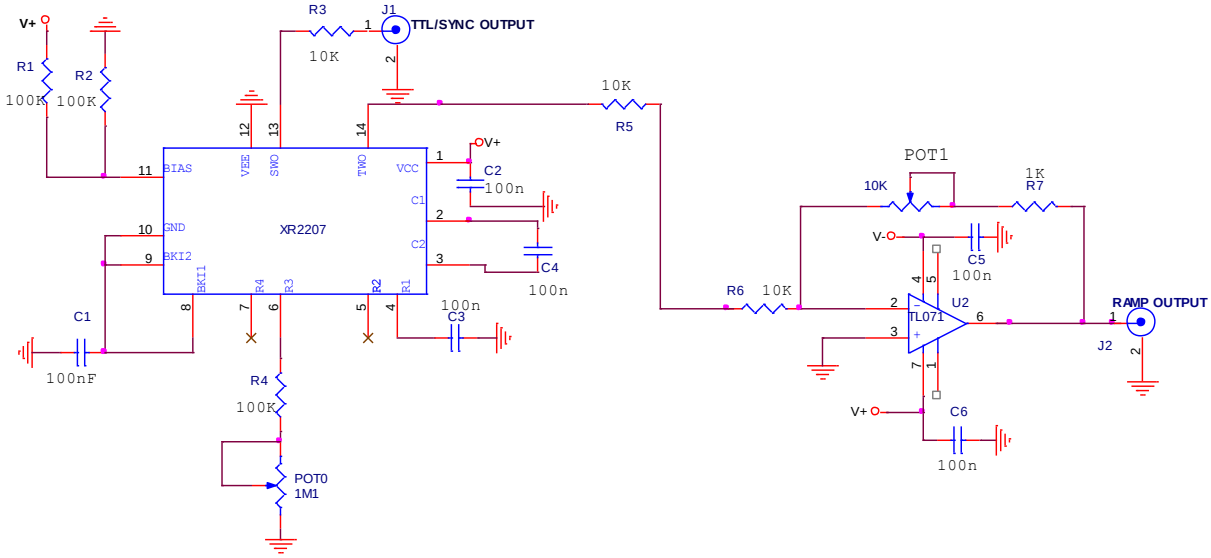

Fig 4.4. Current modulation using IC XR2206

Results:

The figures below show the results of the setup. Waveform (1)- is the output wave forms across the magnetic coil, Waveform(2) is the ramp signal fed to the current programming pins of the power supply and waveform(3) is the Sync output of Ramp & sync generator circuits. We have tested the circuits for various current outputs starting from 1A to 10A and observed that output currents are in sync with the programming analog ramp signal.

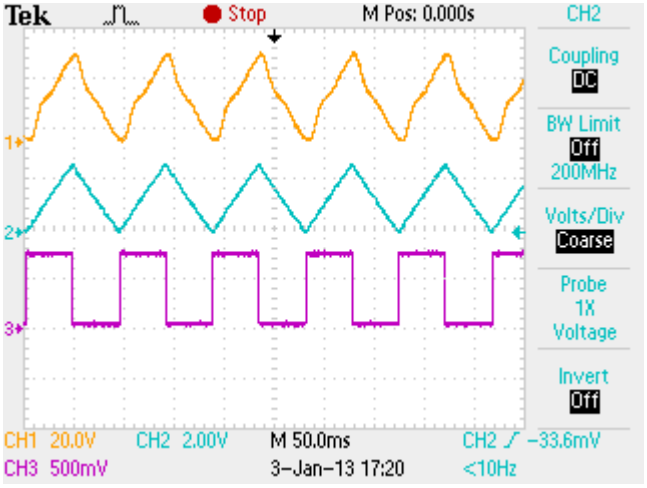

Fig 4.5: Results - Current modulation using IC XR2206

4.2.8. Current modulation using Agilent power supply N5747 programmable DC power supply

We are using Agilent power supply N5747 programmable DC power supply for the Magnetic coil switching circuit. Agilent Technologies Series N5700 System DC Power Supplies are general-purpose, 1U (rack unit) high, switching power supplies that are available with a wide variety of output voltage and current ratings. The output voltage range is 0-60V and output current range is 0-12.5A.

Output Features of N5747 power supply are:

-Constant voltage/constant current with automatic crossover.

-High-resolution voltage and current front panel controls.

-Accurate voltage and current read back.

-Independent edge-triggered external shut-off, and level triggered external enable/disable.

-Parallel master/slave operation with active current sharing.

-Remote sensing to compensate for voltage drop in load leads

– Analog output programming and monitoring.

Programmable Functions of N5757 power supply are:

- Output voltage and current setting.

- Output voltage and current measurement.
- Output voltage and current trigger setting.
- Output On/Off control.
- Over-current protection setting.
- Over-voltage protection setting and read back.
- Under-voltage limit setting and read back.
- Start-up mode (either last setting or reset mode)

In a programmable power supply the output voltage and output current can be programmed. The rear panel of the N5747A as shown in fig 4.6 has connector J1 (5) Analog programming connector, which is a 25 pin D connector. There is 9 position switch SW1 (6) for remote programming and monitoring modes for output volgate, current limit and other control functions[10].

The Rear Panel – At a Glance

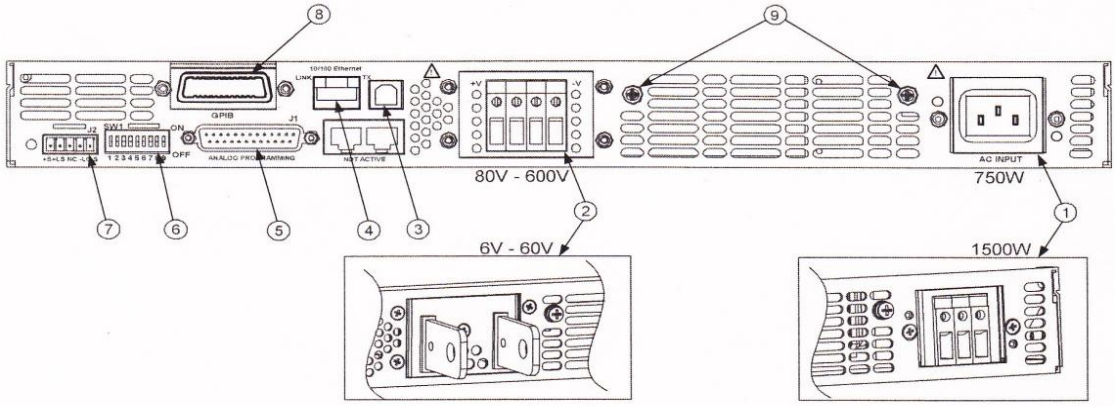

1 – AC input connector	Wire clamp connector for 1500W output models. IEC connector for 750W output models.
2 – DC output connector	Wire clamp connector for 80V to 600V models. Bus bars for 6V to 60V models.
3 – USB connector	Connector for connecting to a USB interface. See chapter 4 for setup.
4 – LAN connector	Connector for connecting to a LAN interface. LINK LED indicates link integrity. TX LED indicates LAN activity. See chapter 4 for LAN setup.
5 – Analog Programming connector	Connector for the analog interface. Includes output voltage and current limit programming and monitoring signals, Shut-Off control (electrical signal), Enable/Disable control (dry-contact), power supply ok (Power Supply OK) signal and operation mode (CV/CC) signal. (See next page for details)
6 – SW1 setup switch	Nine-position switch for selecting remote programming and monitoring modes for Output Voltage, Current Limit and other control functions. (See next page for details)
7 – Remote Sense connector	Connector for making remote sensing connections for regulating the load voltage and compensating for wiring voltage drop. (See next page for details)
8 – GPIB connector	Connector for connecting to a GPIB interface. See chapter 4 for setup.
9 – Ground screw	M4x8 screws for making chassis ground connections

Fig 4.6 Rear panel of the N5747 DC power supply

The details of connector J1 for wiring information in given in fig 4.7. Pins 9 and 10 are used for output voltage and output current programming[10].

J1 Analog Programming Connector

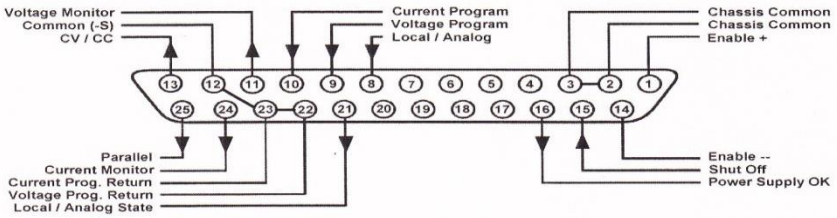

The factory-shipped default configuration is Local operation, which does not require connection to J1.

Pin 1:	**Enable +**	Connect Pin 1 to Pin 14 to enable the output. Disconnect to disable the output.
Pin 2, 3:	**Chassis Common**	Signal return for Pin 15 and Pin 16. Connected to chassis.
Pin 4–7:	**Not Used**	No connection
Pin 8:	**Local/Analog**	Input for selecting between front panel or analog programming of the output.
Pin 9:	**Voltage Program**	Input for voltage or resistance programming of the output voltage.
Pin 10:	**Current Program**	Input for voltage or resistance programming of the output current.
Pin 11:	**Voltage Monitor**	Output for monitoring the output voltage.
Pin 12:	**Common**	Signal return for Pin 8, Pin11, Pin 13, and Pin 24. Connected internally to –S.
Pin 13:	**CV/CC**	Output for constant voltage/constant current mode indication.
Pin 14:	**Enable –**	Connect Pin 14 to Pin 1 to enable the output. Disconnect to disable the output.
Pin 15:	**Shut Off**	Input for Shut-Off control of the output. Referenced to Chassis Common.
Pin 16:	**Power Supply OK**	Output to indicate the power supply status. Referenced to Chassis Common.
Pin 17–20:	**Not Used**	No connection
Pin 21:	**Local/Analog State**	Output for indication of local or analog programming mode.
Pin 22:	**Voltage Prog. Return**	Signal return for Pin 9. Connected internally to –S.
Pin 23:	**Current Prog. Return**	Signal return for Pin 10. Connected internally to –S.
Pin 24:	**Current Monitor**	Output for monitoring the output current.
Pin 25:	**Parallel**	Output for current balancing in parallel operation.

Fig 4.7: Details of J1 connector.

The details of SW1 for selecting different modes of operation are given in figure 4.8.

J2 Sense Connector

1 – Remote sense (+)
2 – Local sense (+)
3 – Not used
4 – Local sense (–)
5 – Remote sense (–)

The factory-shipped configuration is shown in the figure.

SW1 Setup Switch

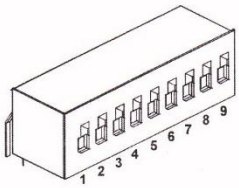

The factory-shipped setting is Down for all switches.

1 – Output voltage, voltage programming	Down: The output voltage is programmed by the front panel. Up: The output voltage is programmed by the external voltage signal.
2 – Output current, voltage programming	Down: The output current is programmed by the front panel. Up: The output current is programmed by the external voltage signal.
3 – Programming range (voltage/resistance)	Down: The remote programming range is: 0 – 5V / 0 – 5KΩ. Up: The remote programming range is: 0 – 10V / 0 – 10KΩ.
4 – Voltage and Current monitoring range	Down: The remote monitoring range is: 0 – 5V. Up: The remote monitoring range is: 0 – 10V.
5 – Shut-Off Logic Select	Down: OUT OFF = Low (0 – 0.6V) or short; OUT ON = High (2V – 15V) or open. Up: OUT OFF = High (2V – 15V) or open; OUT ON = Low (0 – 0.6V) or short.
6 – Not Used	
7 – Output voltage, resistive programming	Down: The output voltage is programmed by the front panel. Up: The output voltage is programmed by the external resistor.
8 – Output current, resistive programming	Down: The output current is programmed by the front panel. Up: The output current is programmed by the external resistor.
9 – Enable/Disable control	Down: The J1 Enable+/Enable– pins are not active. Up: The J1 Enable+/Enable– pins are active.

Fig 4.8. Details of switch SW1

The N57547 power supply requires 5V programming voltage for output voltage (60V) control and 5V for output current (12.5A) control. It has to be scaled according to the output voltage/current requirements.

4.2.9. Current modulation using LabVIEW programs and Agilent Power Supply

In the experimental setup to automate the experiment we are using LabVIEW software based programs from National Instruments to control / automate the experiment. From the main LabVIEW program control signals/triggers signals are given AOMs, Shutters, Camera and Magnetic coils switching circuits. The program gives analog signals to the current programming pins of the Agilent programmable power supply, which drives the magnetic coils and gives TTL signals to the switching circuit.

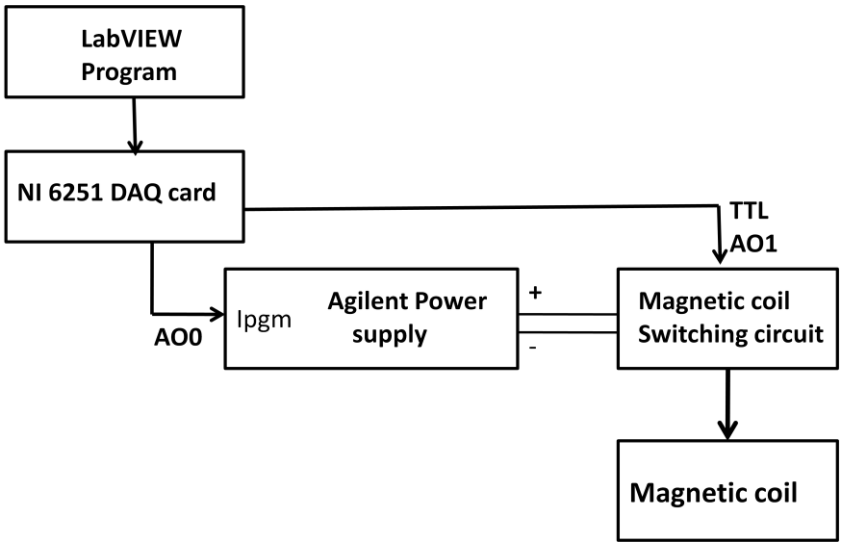

Fig 4.9. Block diagrams of the Magnetic coil switching circuit.

4.2.9.1 LabVIEW AND DATA ACQUISITION SYSTEMS**:**

LabVIEW [Laboratory Virtual Instrumentation Engineering Workbench] is a platform and developmental environment for a virtual programming language from National Instruments. It is a graphical programming environment for data acquisition and control, data analysis and data presentation [11].

It is a graphical language by which code is constructed and saved automatically. There is no text-based code like any other programming language, but a diagrammatic view of how the data flows through the program [11].

LabVIEW is hierarchical in which any virtual instrument that we design (any complete functional unit is called a virtual instrument and is referred to as a “VI” can be quickly

converted into a module which can be a sub-unit of another VI. This is entirely analogous to the concept of a procedure in conventional programming [11].

BASIC CONCEPTS OF LabVIEW :

There are two faces of LabVIEW VI. They are:

i) Block diagram

ii) Front panel

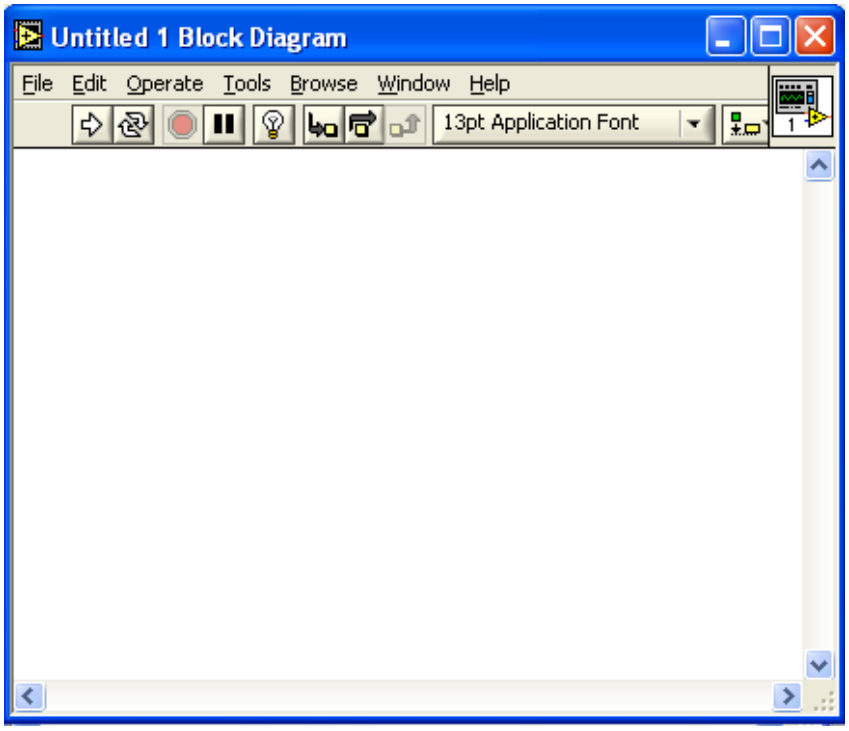

Fig 4.10 : Block diagram of LabVIEW

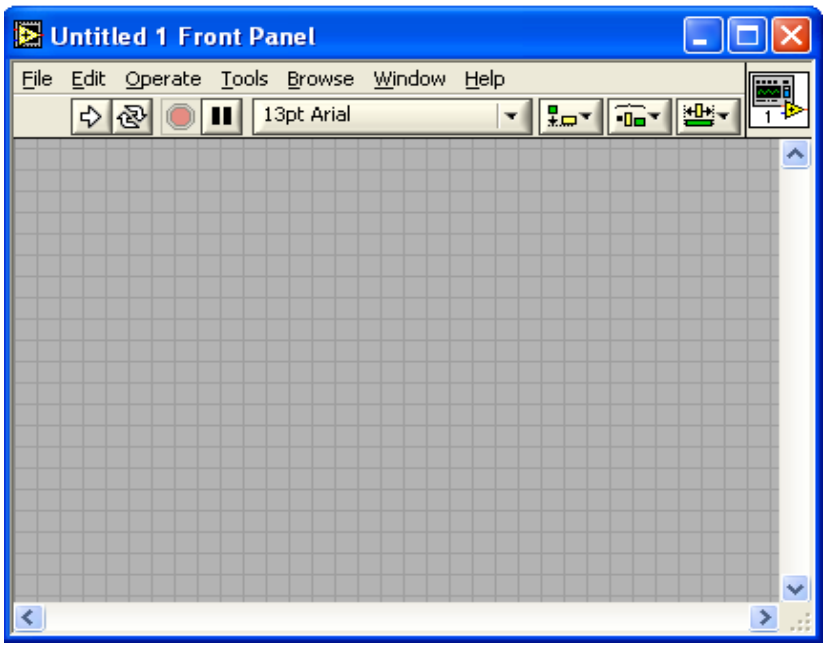

Fig 4.11. Front panel of LabVIEW

The front panel is the face that the user of the system sees. It contains controls and indicators. LabVIEW has a wide range of options to the designer. Controls and Indicators which are important for any LabVIEW programs can be in the form of real controls e.g. knobs, switches etc and Indicators includes graphs and charts [11].

The block diagram of the VI is almost the "backside" of the front panel. It shows how all the controls and indicators fit together as well as the hidden modules where all the work gets done. The concept in LabVIEW is "dataflow" - any item executes when all its inputs are available. This implies Parallelism. One of the major issues in LabVIEW programming is to allocate the timing and ordering of operations. In a conventional programming language this is handled by the order of the statements along with the use of various loop constructs (FOR, WHILE, etc) [12].

4.2.9.2. DATA ACQUISITION (DAQ) SYSTEMS :

Data acquisition (DAQ) is the process of sampling of real world physical conditions and conversion of the resulting samples into digital numeric values that can be manipulated by a computer. Data acquisition and data acquisition systems (DAS) typically involve the conversion of analog waveforms into digital values for processing. The components of data acquisition systems include:

- Sensors that convert physical parameters to electrical signals.
- Signal conditioning circuitry to convert sensor signals into a form that can be converted to digital values.
- Analog-to-digital converters, which convert conditioned sensor signals to digital values.

The DAQ boards (made by National Instruments) are multi-function, plug-n-play, analog and digital input/output boards consisting of an onboard timer, 12 bit analog to digital converter (ADC), 2 digital to analog converters (DAC) and 24 TTL level logic inputs [13].

There are several ways in which the data can be exchanged between instruments and a computer. One way to measure signals and transfer the data into a computer is by using a Data Acquisition board. A typical commercial DAQ card contains ADC and DAC that al-

lows input and output of analog and digital signals in addition to digital input/output channels [13].

SOURCE **:**

Data acquisition begins with the physical phenomenon or physical property to be measured. Examples of this include temperature, light intensity, gas pressure, fluid flow, and force. Regardless of the type of physical property to be measured, the physical state that is to be measured must first be transformed into a unified form that can be sampled by a data acquisition system which is performed by sensors [13].

A sensor which is a type of transducer is a device that converts a physical property into a corresponding electrical signal (e.g., a voltage or current) or into a corresponding electrical characteristic (e.g., resistance or capacitance) that can easily be converted to electrical signal. DAQ systems also employ signal conditioning techniques to adequately modify various different electrical signals into voltage that can then be digitized using an Analog-to-digital converter (ADC) [13].

SIGNALS :

Signals may be digital (also called logic signals) or analog depending on the transducer used. Signal conditioning may be necessary if the signal from the transducer is not suitable for the application being used. The signal may need to be amplified, filtered or demodulated. Various other examples of signal conditioning might be bridge completion, providing current or voltage excitation to the sensor, isolation, and linearization. For transmission purposes, single ended analog signals, which are more susceptible to noise can be converted to differential signals. Once digitized, the signal can be encoded to reduce and correct transmission errors [13].

DAQ HARDWARE **:**

DAQ hardware is interface between the signal and a PC. It could be in the form of modules that can be connected to the computer's ports (parallel, serial, USB, etc…) or cards connected to slots (S-100 bus, AppleBus, ISA, MCA, PCI, PCI-E, etc…) in the mother board. Usually the space on the back of a PCI card is too small for all the connections

needed, so an external breakout box is used. DAQ cards often contain multiple components (multiplexer, ADC, DAC, TTL-IO, high speed timers, RAM) [13].

DAQ SOFTWARE **:**

DAQ software is needed for the DAQ hardware to work with a PC. The device driver performs low-level register writes and reads on the hardware, while exposing a standard API (Application Program Interface) for developing user applications [13]. The functions of DAQ software are

- Acquire data at specified sampling rate.
- Acquire data in the background while processing in foreground.
- Stream data to and from disk.
- Integrate different DAQ boards in a computer and use various functions of a DAQ board from a single user interface.

4.2.9.3. A COMPETE DAQ SYSTEM WITH LabVIEW :

Fig 4.12 : A complete DAQ system with LabVIEW

The figure 4.12 shows a complete DAQ system with LabVIEW. The driver software is a lower level driver that interfaces LabVIEW software with the DAQ boards. LabVIEW identifies each board by a device number, and depending on the chassis of the mother board we can have many DAQ cards. LabVIEW can also combine and display inputs from various sources like inputs from serial and parallel port, data acquisition boards, and GPIB boards on a single interface [13].

NI M series DAQ cards:

NI M Series technology provides more performance, more accuracy, and more I/O than other data acquisition devices. M Series multifunction DAQ devices are well-suited for a wide range of applications in test, control, and design, including automated test, process control, prototype verification, and sensor measurement [14].

The general features of M series DAQ cards are:

- 16- or 18-bit, up to 1.25 MS/s, up to 80 analog inputs
- Up to 4 analog outputs at 16 bits, 2.8 MS/s (2 µs full-scale settling)
- Up to 48 TTL/CMOS digital I/O lines (up to 32 hardware-timed at 10 MHz)
- Two 32-bit, 80 MHz counter/timers

- NI-DAQmx driver software and NI LabVIEW Signal Express for interactive data-logging software
- NI-MCal calibration technology for improved measurement accuracy by up to 5X

In our setup we are using NI High speed M series 6251 DAQ card for automating the experiment.

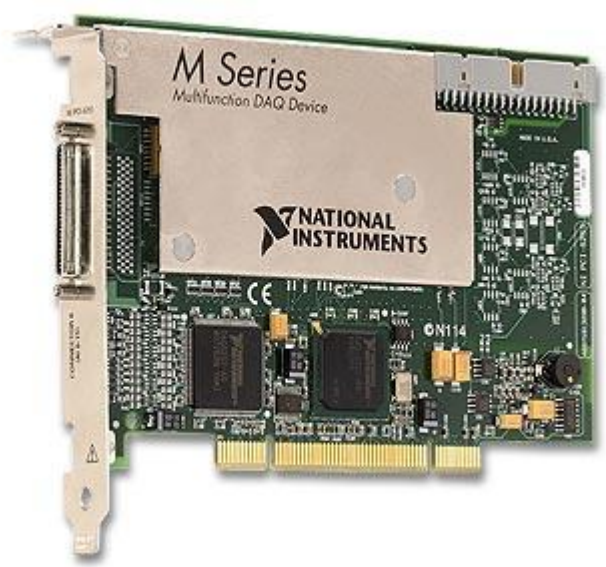

Fig 4.13. M series NI DAQ card

The features of NI DAQ M series 6251 are [14]:

- 16, 32, or 80 analog inputs at 16 bits, 1.25 MS/s (1 MS/s scanning, NI 6255 specified at 750 kS/s scanning)
- Up to 4 analog outputs at 16 bits, 2.8 MS/s (2 µs full-scale settling)
- 7 programmable input ranges (±100 mV to ±10 V) per channel
- Up to 48 TTL/CMOS digital I/O lines (up to 32 hardware-timed at 10 MHz)
- Two 32-bit, 80 MHz counter/timers
- Analog and digital triggering
- X1, X2, or X4 quadrature encoder inputs

4.2.9.4. LabVIEW programs:

The Front panel and Block diagrams screens of the final LabVIEW program are as follows:

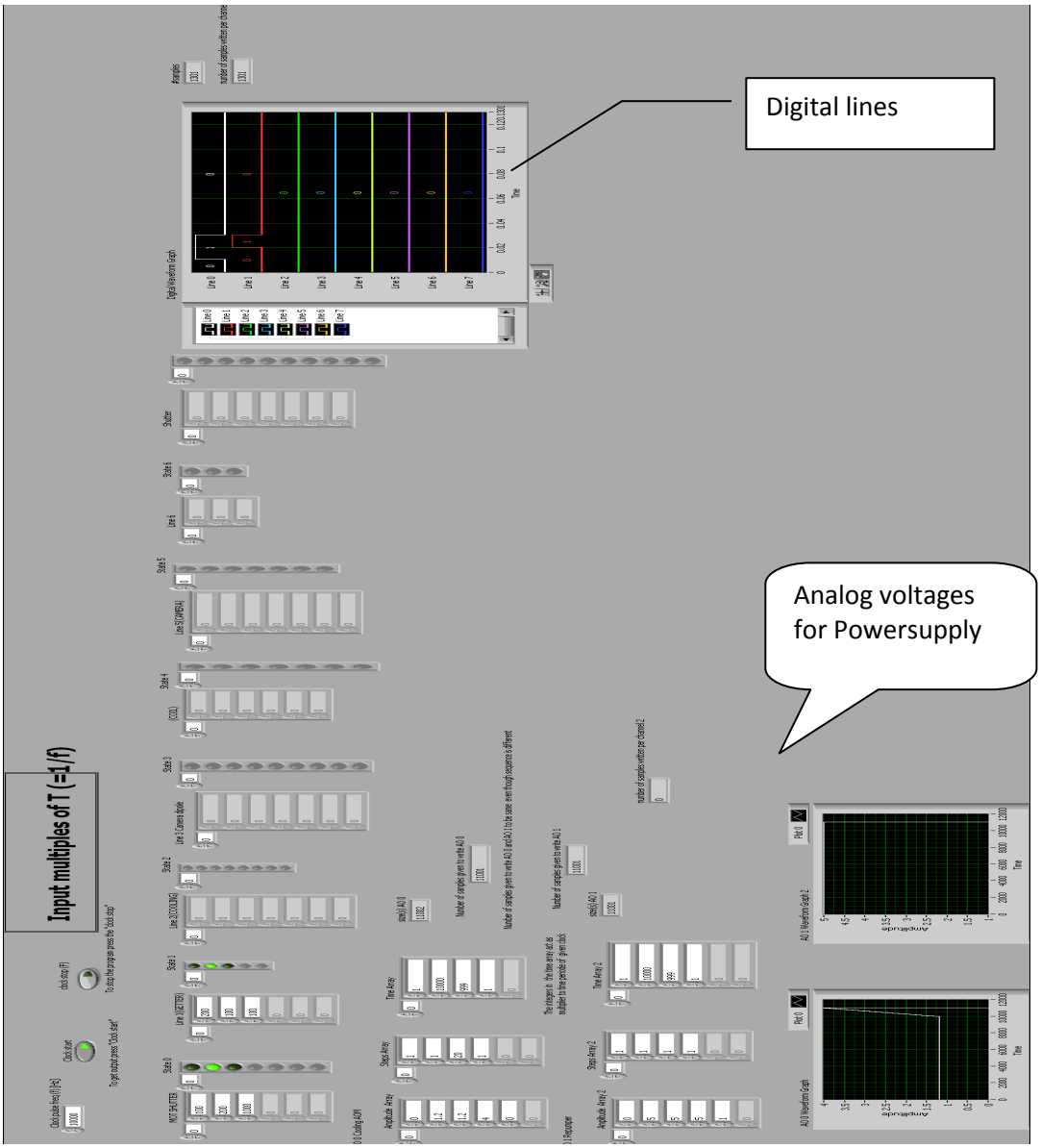

Fig 4.14. Front panel of the Main control program for automation of the experiment

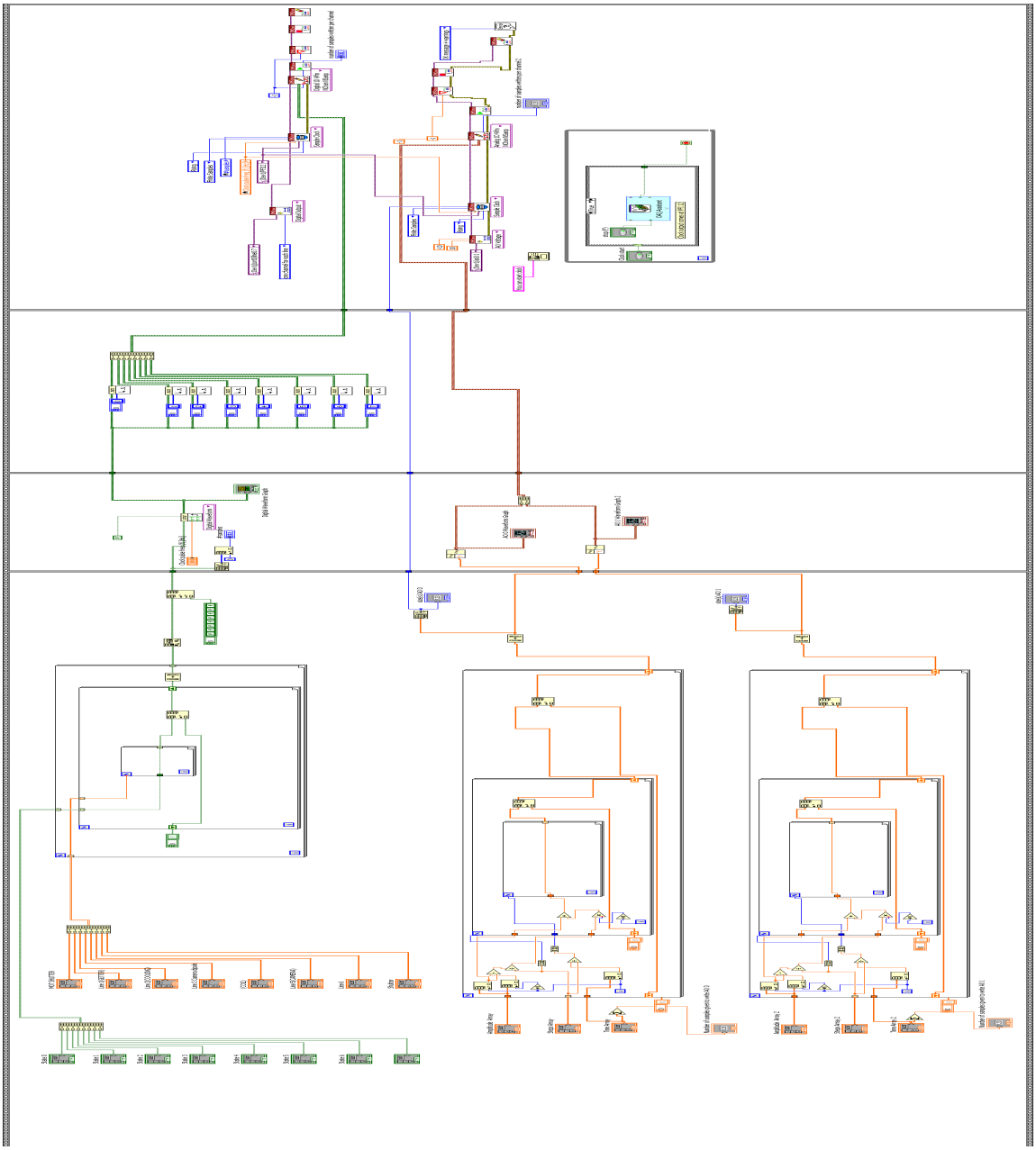

Fig 4.15: Block diagram of the Main control program for automation of the experiment

The main LabVIEW control program has eight digital outputs and two analog outputs. For digital outputs each output can be programmed for required logic states, on and off durations up to few microseconds. This is achieved by initially creating arrays for logic states (ON/OFF) and durations for each state in terms of milli seconds. These two data are combined to forms arrays and finally a 2D array is derived for all the digital channels in a “digital waveform form” data type format.

Measurement I/O VIs (which comes under Block diagram) are used to interface with NI DAQ, NI DAQmx and other data acquisition systems. We use DAQmx - Data Acquisition VIs to develop instrumentation, acquisition, and control applications. The 2D array is converted into a Digital waveform using DWDT Boolean Array to Digital.VI, which will have logic state and duration of each state for all the digital lines. Then using DAQmx VIs namely DAQmx create, DAQmx timing, DAQmx Write, DAQmx Start, DAQmx Wait until done, DAQmx stop and DAQ clear, the digital data is written into all channels at the click on the "Start clock" button on front panel. We have chosen Port 0, line 0 to 7 of Device1 which is PCI 6251 DAQ card. This ensures that all the digital channels are synchronized to a common clock.

For analog outputs, depending on the output waveform pattern required, amplitude levels, step size and durations for each level can be programmed as per our requirements for an experiment. The AO0 and AO1 are the analog ports of NI 6251 card used for analog outputs. Data for both the channels are combined in an array, and a "Waveform (DBL)" data type format is derived. Using Measurement I/O VIs and DAQmx VIs final data is written into analog channels AO0, AO1 of PCI 6251 DAQ card which are synchronized to a common clock.

We have programmed the outputs as per the values shown in the figure below (figure 4.16) and figure 4.17 shows the analog outputs of the LabVIEW main program measured on an oscilloscope.

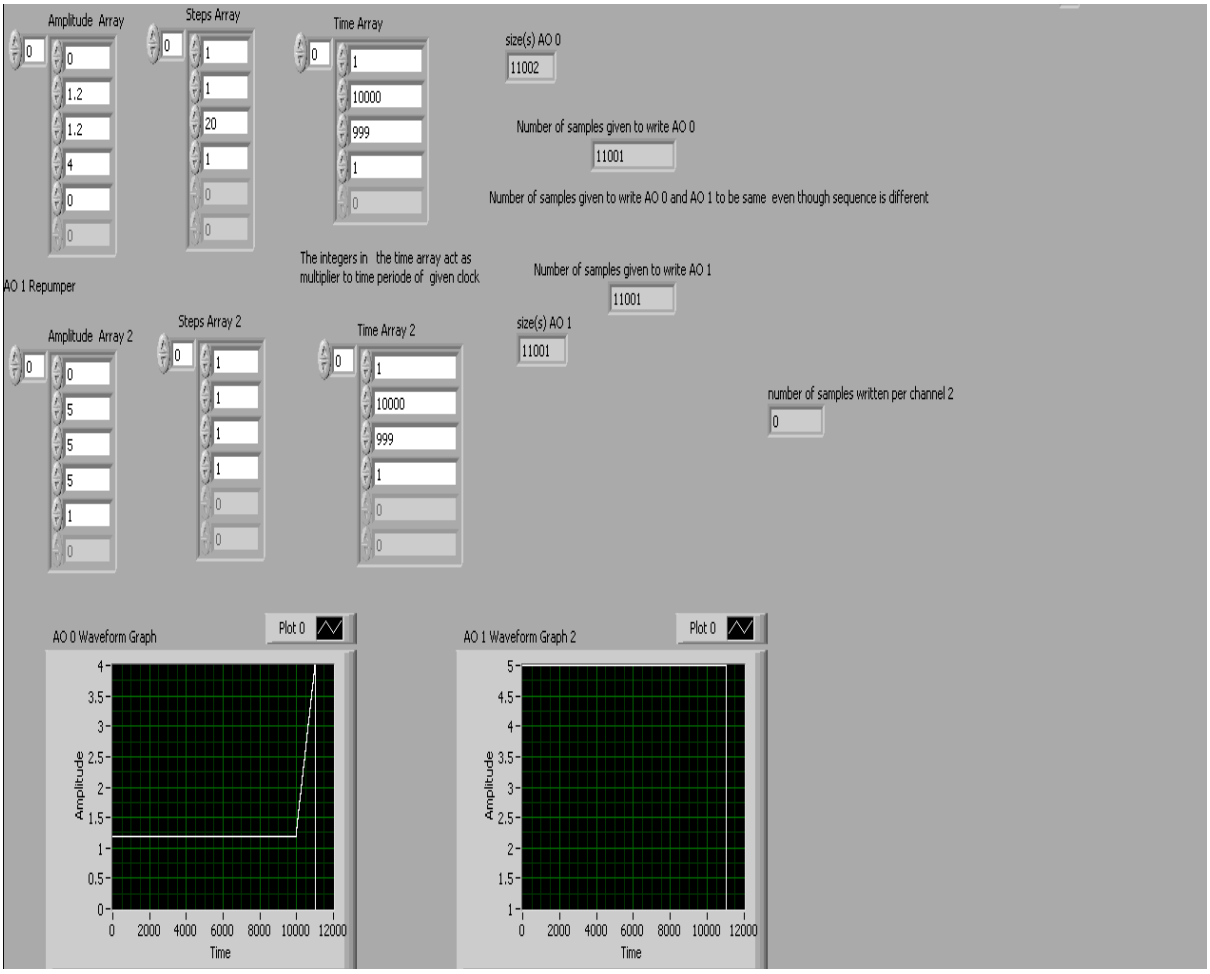

Fig 4.16: Analog output voltages from the LabVIEW programs

4.2.9.5. DAQ card 6251 analog outputs:

Figure 4.17 shows the analog outputs from AO0 and AO1 from the DAQ card 6251 recorded on the oscilloscope, which are fed to the current programming pins of the power supply and IGBT gate circuit.

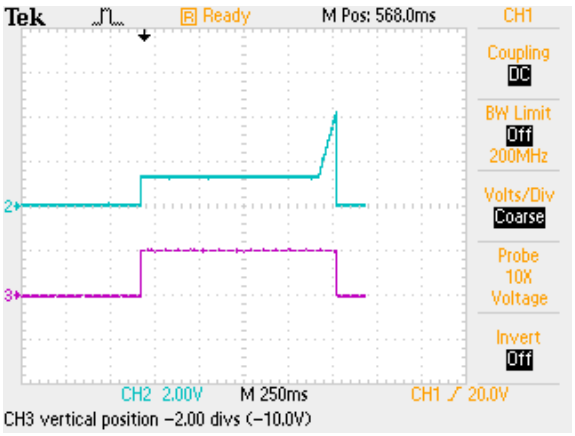

Fig 4.17: Analog output voltages from AO0(ch2) and AO1(ch3) of 6251 DAQ card

4.2.9.6. Results - Magnetic coil switching circuit outputs:

AO1 and AO0 outputs are fed to the Switching circuit and current programming pins of the Agilent power supply. Based on the instantaneous values of programming voltages (0-5V), the power supply output current (0 – 12.5A) will change, when the IGBT is turned on.

The initial measurements across small resistance (Rsense) (ch1) which is in series with the load , current programming voltages fed the power supply (ch2) and TTL signals (ch3) voltages are shown in the figures below (4.18,4.19 and 4.20).

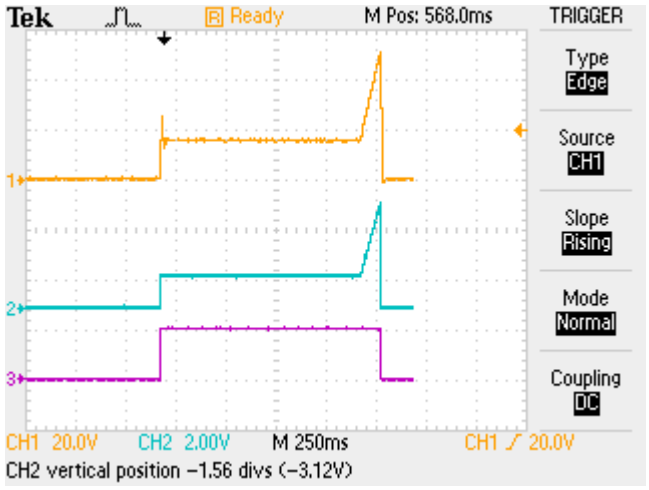

Fig 4.18. Measurements1 across Rsenseresistor (CH 1)

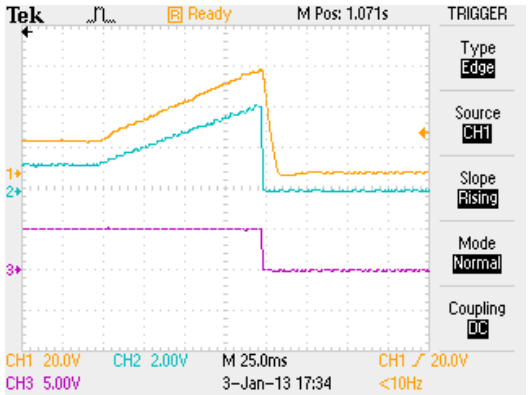

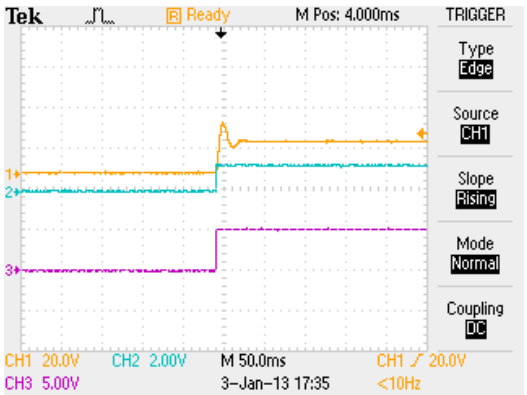

Fig 4.19. Fall time1 measurements (CH 1)

Fig 4.20. Rise time1 measurements (CH 1)

From the graphs we observe switching of currents is in synchronous with the programming voltages. We observe that there are overshoots, and ringing effects which can ac-

tually disturb the experimental results, as the cold cloud is very sensitive to the location of magnetic field zero.

To overcome the overshoot and ringing effect, the RLC parameters of the magnetic coil circuitry are varied by connecting low value thick film resistor (LTO 100 from Vishay semiconductor) which has low inductance, resistance (1 ohm to 2 ohms) in series with the magnetic coil i.e. one end of the thick film resistor is connected to the coil and other end to the collector of IGBT (Figure 4.3 a). The following figures (4.21, 4.22 and 4.23) show the results of the switching circuits with low value thick film resistor and with better performance.

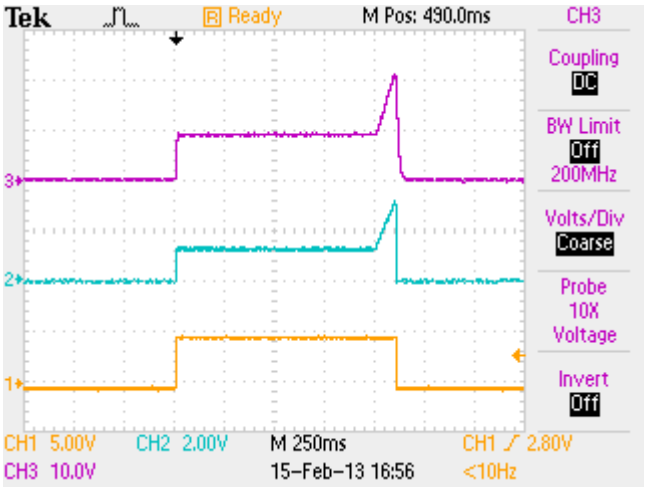

Fig 4.21. Measurements2 across Rsense resistor (CH3)

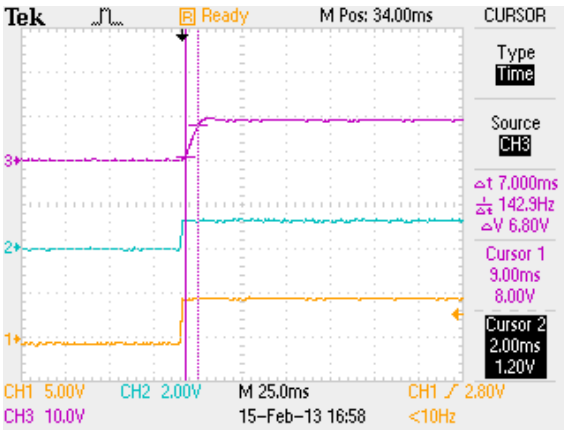

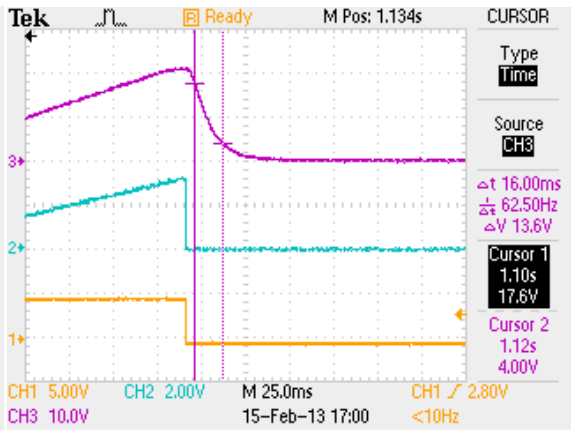

Fig 4.22. Rise time2 measurements (CH 3) Fig 4.23. Fall time2 measurements (CH 3)

The delay in rise time and fall time is observed to be about 7ms and 16 ms, after tuning the RLC parameter of the freewheeling circuit. The parameters are best tuned in the experimental setup, while performing measurements in the lab.

4.3. MOT oscillating circuits

Cold atoms produced by laser cooling and trapping techniques are used widely for high precision experiments like high resolution spectroscopy, precision measurements, accurate atomic clocks, quantum information, quantum entanglement of atoms, single atom traps etc. To perform such highly precise experiments with cold atoms one needs an accurate characterization of the cold atoms.

Temperature of the cold atoms is an important characteristic physical quantity which is very useful in performing such accurate experiments mentioned above.

The various methods to measure the "temperature" of the cold atoms are

a. The Time of Flight (TOF) method: In this method the trapping laser beams are turned off for several ms, so that atoms move freely during this flight time and at the same time fall under force of gravity. Then the trapping laser beams are switched on and an image of the cloud is taken with CCD camera. The size and the displacement of the MOT under gravity give an estimate of the temperature.

b. The Release Recapture method: This method measures the number of atom that escaped in a time interval when the atoms are temporarily free. Both trapping and repumper laser have to be turned off for a very short time interval. The difference in luminescence before and after this interval is a measure for the amount of escaped atoms. From this amount the average velocity can be determined. An AOM (Acousto-Optic Modulator) is generally used to switch off and on both the laser beams for a very short time interval.

c. Absorption imaging method: In this method the size of the MOT is calculated with the help of absorption image obtained from the CCD camera. The rest of the procedure is

same as release and recapture method. In this method also the temperature calculation is done with the help of AOMs as done in the release and recaptures method.

d. Trap Oscillation Method: In this method the temperature, spring constant, friction coefficient can be measured non-destructively. The trap centre (zero point of the magnetic field) is changed with the use of an extra Helmholtz coil in which a periodically modulated current is passed. The first three methods are destructive in nature, as we need to switch off the magnetic coils which will cause the MOT to disappear.

The first three methods give a very accurate measurement of the temperature but, the magnetic field has to be switched off very fast during the period that the laser beams are switched off. As the MOT coils have a response time which limits our ability to switch the coils on and off. If these measurements are done without switching off the magnetic fields, the atoms will be confined in a potential well caused by the magnetic field.

4.3.1. Experimental Setup for Trap oscillation method:

The setup for the Trap oscillation method is as show in fig 4.24. The new addition to the existing Laser cooling and trapping setup is an extra pair of coil Helmholtz configuration. The basic components of the setup are:

1. Signal generator – for producing the modulating signal
2. Power amplifier – for amplifying the modulating signal to drive the magnetic coil
3. Femto watt detector – for imaging the MOT
4. Lock-in amplifier (SRS 850) - for lock-in detection of the detector signal
5. MOT (Magneto-optic trap) coils – indicated as M
6. A pair Compensating coil - indicated as C

4.3.2. Trap Center Oscillation Method

At the center of the MOT chamber we have the zero point of the quadrupole magnetic field produced by the MOT coils (M). This zero point is oscillated using a pair of Helmholtz coils (compensating coils, C) placed on either ends of MOT chamber. This coil has 11 turns and an impedance of about 1 ohm. Signal generator DS345 is used to generate

the modulating signal for the amplifier. The Power amplifier (OPA 541) is used the drive the compensating coils up to currents 2A.

Femto watt detector is placed closed to the experimental chamber to image the cold cloud of atoms. As the zero of the trap center is oscillated by the amplifier circuit, Femto watt detector detects this change in intensity. This signal is fed as signal input to the Lock-in amplifier for the Lock-in detection. It is essential to do the Lock-in detection, as the signal from the femto watt detector is very weak, and noisy because of background light, reflections, and scattering from other parts of the chamber. The reference signal for lock-in amplifier can be from the TTL output of the signal generator or voltage drop across R connected in series with the compensating coils C. The lock-in amplifier once locked with the external reference signal displays the phase difference between the reference signal and the input signal.

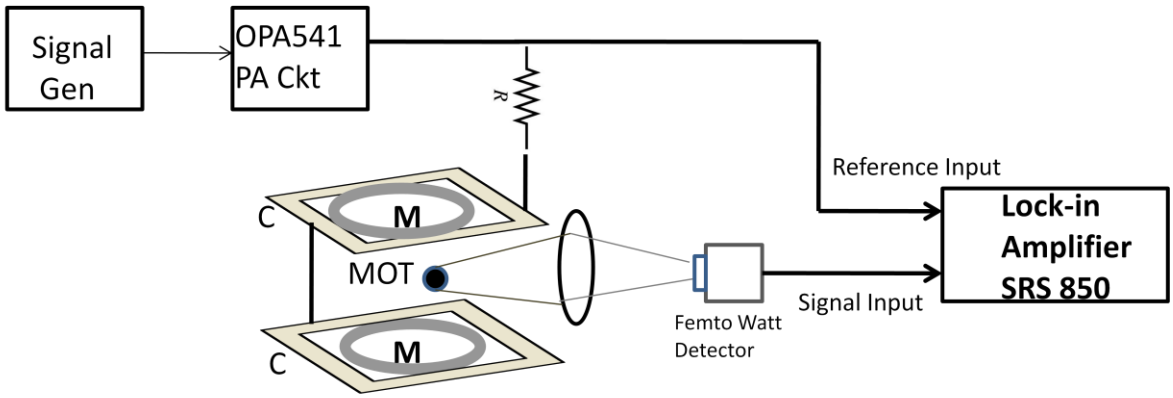

M-MOT coils
C- Compensating coils

Fig 4.24. Experimental setup for Trap oscillation method

4.3.3. OPERATIONAL AMPLIFIERS

An operational amplifier, is often called an op-amp, is a DC-coupled high-gain electronic voltage amplifier with a differential input and usually a single-ended output. An op-amp produces an output voltage very much larger than the voltage difference between its input terminals.

The op-amp's large gain is controlled by negative feedback which determines the magnitude of its output ("closed-loop") voltage gain in amplifier applications or the transfer function required (in analog computers). The important characteristics of an op-amp are high input impedance (ideally infinite), low output impedance (ideally zero)[12].

4.3.3.1. POWER OPERATIONAL AMPLIFIERS:

Power operational amplifiers (POA) are used to increase the power of low-level signals in applications that drive low impedances or reactive loads. They dissipate excess energy as heat, deliver extensive current and can sustain relatively high supply voltages. Most devices have impedances that are 10 to 100 times lower than small-signal operational amplifiers and can deliver larger amounts of current and dissipate more power. There are several operational classes for power operational amplifiers. Class A devices are the most linear and the least efficient. Class AB designs provide increased efficiency and excellent linearity. Class B amplifiers are used almost exclusively in low-power applications. Class C devices are used with radio frequency (RF) transmissions. Class D amplifiers switch on and off at least two times per cycle [15].

Important specifications of Power operational Amplifiers are: Output peak current, Output voltage swing, Open-loop gain, Gain bandwidth product, Slew rate, Common mode rejection ratio (CMRR), Input offset voltage, Input bias current, Input impedance and other performance specifications for power operational amplifiers include supply voltage range, internal power dissipation, quiescent current, and power bandwidth [15].

Features for power operational amplifiers include on-chip electrostatic discharge (ESD) protection, rail-to-rail outputs, and embedded current limits[15,16].

4.3.3.2. OPERATIONAL POWER AMPLIFIERS (OPA 541) :

The OPA541 is a power operational amplifier capable of operation from power supplies up to +/-40V and delivering continuous output currents up to 5A. Internal current limit circuitry can be user-programmed with a single external resistor, protecting the amplifier and load from fault conditions. The OPA541 is fabricated using a bipolar / FET proc-

ess. Pinout is compatible with popular hybrid power amplifiers such as the OPA511, OPA512[18].

The OPA541 uses a single current-limit resistor to set both the positive and negative current limits. The OPA541 is available in an 11-pin power plastic package (fig 4.26) and an industry-standard 8-pin TO-3 hermetic package. The power plastic package has a coppe- lead frame to maximize heat transfer. The TO-3 package is isolated from all circuitry, allowing it to be mounted directly to a heat sink without special insulators [18].

PIN OUT Top View

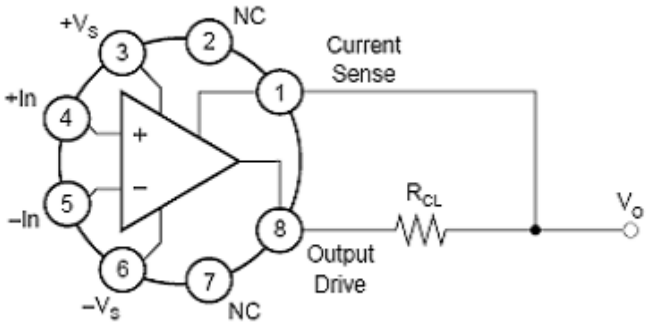

Fig 4.25.Pinout showing top view of OPA541

Plastic Package

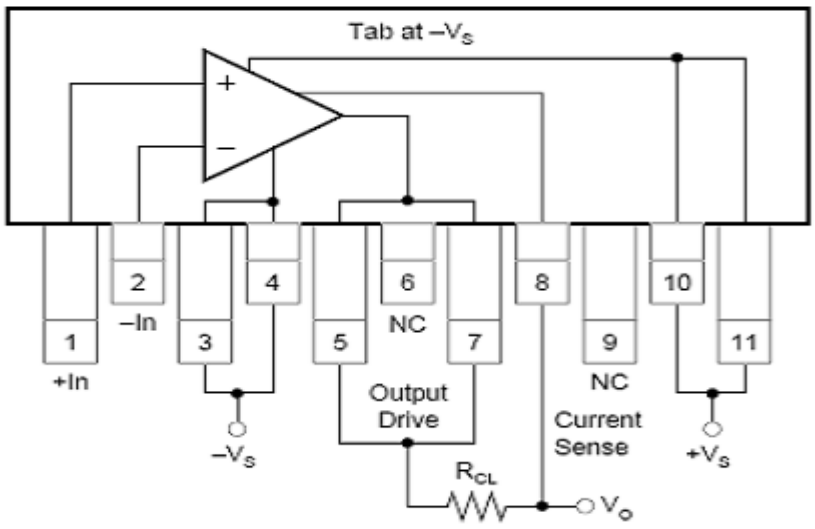

Fig 4.26. Pin out showing the plastic package of OPA541

4.3.3.3. Circuit Diagram of OPA 541

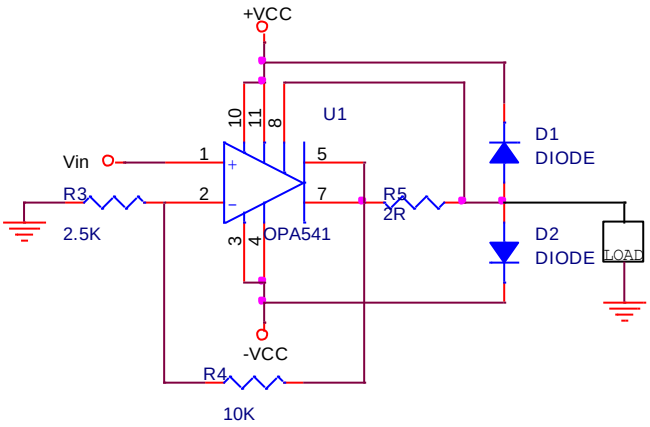

Fig 4.27.Circuit diagram of OPA541

DESIGN :

Gain , Av = $1 + R_2 / R_1$, ----(4)

Let, Av = 20, Select, R_2 = 10 KΩ, therefore R_1 = 2.5 KΩ ----(5)

POWER SUPPLIES:

The OPA541 is specified for operation from power supplies up to +/-40V. It can also be operated from unbalanced power supplies or a single power supply, as long as the total power supply voltage does not exceed 80V. The power supplies is bypassed with low series impedance capacitors such as ceramic or tantalum and is located as near as practical to the amplifier's power supply pins[18].

4.3.3.4. Current Limit design for OPA541

Internal current limit circuitry is controlled by a single external resistor, R_{CL}. Output load current flows through this external resistor. The current limit is activated when the voltage across this resistor is approximately a base-emitter turn-on voltage. The value of the current limit resistor is approximately :R_{CL}

$$Rcl = \frac{0.813}{Ilim} - 0.02 \quad \text{----(6)}$$

Because of the internal structure of the OPA541, the actual current limit depends on whether current is positive or negative. The above R_{CL} gives an average value. For a given R_{CL}, $+I_{OUT}$ will actually be limited at about 10% below the expected level, while $-I_{OUT}$ will

be limited about 10% above the expected level. The current limit value decreases with increasing temperature due to the temperature coefficient of a base-emitter junction voltage and the current limit value increases at low temperatures.

HEAT SINKING:

Power amplifiers are rated by case temperature, not ambient temperature as with signal op amps. Sufficient heat sinking must be provided to keep the case temperature within rated limits for the maximum ambient temperature and power dissipation. The thermal resistance of the heat sink required is calculated by [18].

$\theta_{HS} = (T_{CASE} - T_{AMBIENT}) / P_D(max)$ ----(7)

4.3.3.5. Output Characteristics of Power Amplifier OPA541:

i) AMPLITUDE Vs FREQUENCY PLOT

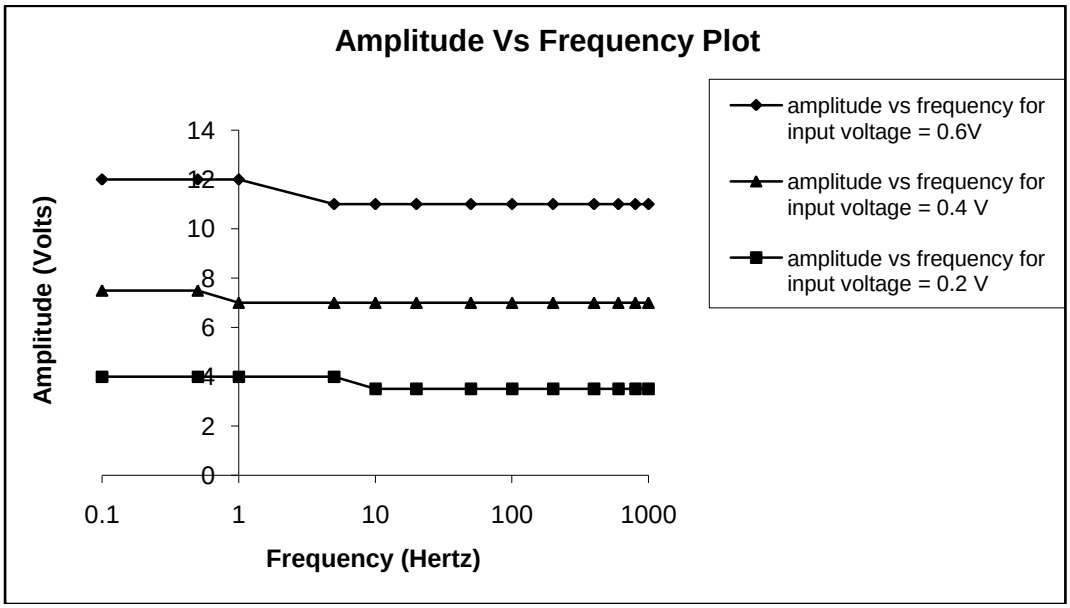

Fig 4.28. Amplitude Vs. Frequency Plot of OPA541

Figure 4.28 shows the output characteristics of power amplifier with amplitude Vs. frequency curve for different input voltages such as 0.6V, 0.4V and 0.2V. The amplifier output voltage ranges from 0 to 14V and the frequency ranges from 0.1 to 1000 Hz. For Trap Oscillation experiments it is required to maintain the output amplitude level constant over a range of frequencies for given input amplitude.

4.4. Lock-in detection:

For Lock-in detection of the detector signal, the output of the detector is fed as the signal input to the Lock-in amplifier and the voltage across the resistor R is fed as the reference input to the lock-in amplifier.

4.4.1. Lock-in amplifier:

A lock-in amplifier (also known as a phase-sensitive detector) is a type of amplifier that can extract a signal with a known carrier wave from an extremely noisy environment (the signal-to-noise ratio can be -60 dB or even less). The device is used to measure phase shift, even when the signals are large and of high signal-to-noise ratio. Recovering signals at low signal-to-noise ratios requires a strong, clean reference signal at the same frequency as the input signal.

4.4.2. Basic Concept of Lock-in amplifier:

Operation of a lock-in amplifier relies on the orthogonality of sinusoidal functions. When a sinusoidal function of frequency v is multiplied by another sinusoidal function of frequency μ not equal to v and integrated over a time much longer than the period of the two functions, the result is zero. In the case when μ is equal to v, and the two functions are in phase, the average value is equal to half of the product of the amplitudes.

Lock-in amplifier (also known as phase sensitive detector) takes the input signal, multiplies it by the reference signal (either provided from the internal oscillator or an external source), and integrates it over a specified time, usually on the order of milliseconds to a few seconds. The resulting signal is a DC signal, where the contribution from any signal that is not at the same frequency as the reference signal is attenuated close to zero, as well as the out-of-phase component of the signal that has the same frequency as the reference signal (because sine functions are orthogonal to the cosine functions of the same frequency).

A lock-in amplifier has special rectifier, called a phase-sensitive detector (PSD), which performs this AC to DC conversion. It rectifies only the signal of interest while suppress-

ing the effect of noise or interfering components which may accompany that signal. So in a lock-in amplifier the final output is not affected by the presence of noise in the applied signal. A reference voltage of the same frequency and with a fixed phase relationship to that of the signal is given as an input to the Lock-in amplifier. The use of such a reference signal ensures that the instrument will "track" any changes in the frequency of the signal of interest, since the reference circuit is "locked" to it. Because of the automatic tracking, lock-in amplifiers can give effective "Q" values (a measure of filter selectivity) in excess of 100,000, whereas a normal bandpass filter becomes difficult to use with Q's greater than 50[19].

4.4.3. Phase-Sensitive Detection

Phase-sensitive detector (PSD) is the heart of Lock-in amplifier, also known as a demodulator or mixer. The detector operates by multiplying two signals "Signal In" and Reference signal" together. The mean level is:-

-- proportional to the product of the signal and reference frequency amplitudes

-- related to the phase angle between the signal and reference.

The mean level is a DC component of the demodulator output. It is isolated by using a low-pass filter. The filtered output is then measured using conventional DC voltmeter techniques. The noise, which by definition has no fixed frequency or phase relationship to the reference, is also multiplied by the reference signal in the demodulator, but does not result in any change to the mean DC level. Noise components at frequencies very close to that of the reference do result in demodulator outputs at very low frequencies, but by setting the low-pass filter to a sufficiently low cut-off frequency these can be rejected. Hence the combination of a demodulator and low-pass output filter allows signals to be measured even when accompanied by significant noise [20,21].

The mathematical analysis is as follows:

Consider the case where a noise-free sinusoidal signal voltage Vin is detected, where

$$Vin = A\cos(\omega t) \qquad \text{----(7)}$$

ω is the angular frequency of the signal which is related to the frequency F, $\omega = 2\pi F$

The lock-in amplifier is supplied with a reference signal at frequency F derived from the same source as the signal, and uses this to generate an internal reference signal of:

$Vref = B\cos(\omega t + \theta)$, ---- (8)

where θ is a user adjustable phase shift introduced within the lock-in amplifier.

The detection process consists of multiplying these two components together, the PSD output voltage is given by

$$Vpsd = A\cos(\omega t).Bcos(wt + \theta) \quad \text{----(9)}$$

$$= AB\ cos\omega t\ (\cos\omega t\ cos\theta - sin\omega t\ sin\theta) \quad \text{---- (10)}$$

$$= AB\ (\cos 2\omega t\ cos\theta - coswt\ sin\omega t\ sin\theta) \quad \text{---- (11)}$$

$$= AB\ ((\tfrac{1}{2} + \tfrac{1}{2}\cos 2\omega t)cos\theta - \tfrac{1}{2}\sin 2\omega t\ sin\theta) \quad \text{---- (12)}$$

$$= \tfrac{1}{2}\ AB((1 + cos2\omega t)cos\theta - \sin 2\omega t\ sin\theta\ ) \quad \text{---- (13)}$$

$$= \tfrac{1}{2}AB((\cos\theta + \cos 2\omega\ cos\theta - \sin 2\omega t\ sin\theta) \quad \text{---- (14)}$$

$$= \tfrac{1}{2}AB\ cos\theta + \tfrac{1}{2}AB\ (\cos 2\omega t cos\theta - \sin 2\omega t\ sin\theta) \quad \text{---- (15)}$$

$$= \tfrac{1}{2}\ AB\ cos\theta + \tfrac{1}{2}AB\cos(2\omega t + \theta) \quad \text{---- (16)}$$

If the amplitude B, of the reference frequency is kept constant, then the output from the PSD is a DC signal which is

-- Proportional to the magnitude of the input signal A

-- Proportional to the cosine of the angle θ, between it and the reference signal

-- modulated at 2ωt, i.e. it contains components at twice the reference frequency

The output from the PSD passes through a low-pass filter which removes the 2ωt component, leaving the output of the lock-in amplifier as the required DC signal.

Usually the signal will be accompanied by noise, but it can be shown that as long as there is no consistent phase relationship between the noise and the signal, the output of the multiplier due to the noise voltages will not be steady and can be removed by the output filter[20].

4.4.4. The Typical Lock-In Amplifier

The block diagram of a typical lock-in amplifier is shown in figure 4.29.

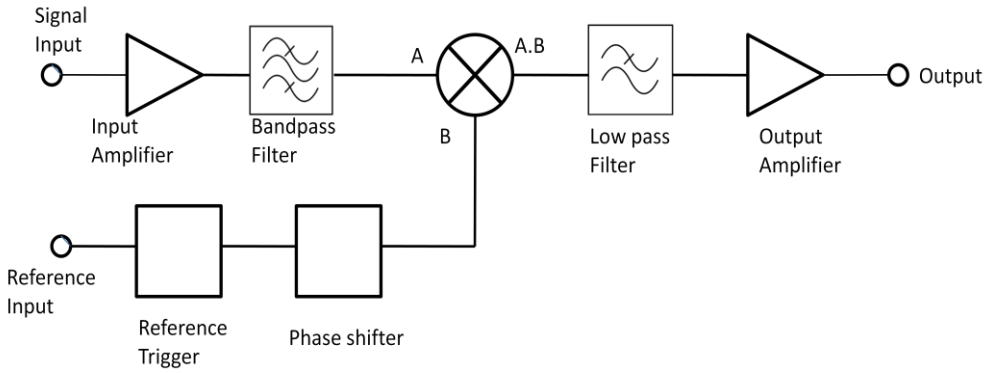

Fig 4.29. Block diagram of Lock-in Amplifier

The output from a lock-in amplifier is a DC voltage which was usually displayed on an analog panel meter. For analog form of outputs, phase-sensitive detector uses an ADC to generate their digital output, whereas digital multiplying lock-in amplifiers use a digital to analog converter (DAC) to generate the analog output[20].

4.4.5. Time Constant of a Lock-in Amplifier

While using a lock-in amplifier, as the input signal frequency is increased/decreased, then accordingly the time constant must be adjusted. The time constant defines the band width over which the lock-in amplifier needs to scan and reference it with the reference signal. Usually, the time constant is set equal to or greater than the frequency of the input signal.

4.4.6. Experimental Setup for Trap Center Oscillation

The setup has only a few additions to the already existing Laser Cooling and Trapping setup. An extra pair of coils in Helmholtz configuration is used. The modulation to the input current is given with the help of a signal generator. The detection system used for detecting the modulation of the MOT is a femto-watt detector.

Trap Center Oscillation

The zero point magnetic quadrupole field is oscillated using an extra coil which is placed on either ends of the MOT chamber. The signal generator feeds modulating input to OPA 541 current modulation circuit, which modulates the current in the coil according to the function which is fed.

The cold atoms scatter the laser light, which is imaged using the Femto-Watt detector. As the zero point of the quadrupole magnetic field is oscillated, the intensity of light being imaged by the detection region of the femto-watt detector changes as the MOT oscillates. The signal from the femto-watt detector is used as an input to the lock-in amplifier along with a reference signal.

A femto-watt detector is used to detect signals which are very weak. In this case the signal from the femto-watt cannot be seen clearly in an oscilloscope at high frequencies due to the noise in the signal. Such signals can be only be detected with the help of lock-in detection technique, using a Lock-in amplifier. The voltage drop across the resistor R or an TTL pulse output from the signal generator can be used as a reference signal for the lock-in amplifier. The lock-in amplifier once locked with the external reference signal displays the phase difference between the reference signal and the input signal.

4.4.7. Results

We have measured and tabulated the phase difference (ϕ) between the input signal and the reference signal over frequencies from 1Hz to 100Hz for different sets of data (figure 4.30). Input signal is from the femto watt detector which is imaging the MOT which is oscillating, and the reference signal measured across resistor R.

Acousto optic modulators (AOM) are used to introduce frequency shifts in the cooling laser beams, which can be tunable over large frequencies. At a given frequency of the AOM or laser detuning, the frequency of modulating signal from signal generator is varied from 1 Hz to 100 Hz, and phase difference (ϕ) between the input signal and the reference signal is tabulated and plotted as shown in figures 4.30.

With the help of curve fitting and measuring the modulating signal frequency when the phase(ϕ) is 90 degrees, amplitude A as a function of ω, one can yield the constants ά (absorption coefficient) and *k* (kappa*).* Using these constants we can calculate the temperature T of the cold cloud using the following formula

$$k_B T = \frac{1}{2} k(x)^2 \qquad \text{--------(17)}$$

where k_B=Boltzmann constant (1.38*10^{-23} joules/Kelvin), where x is the average displacement of the cloud.

The main aim of the experiment was not only to measure the temperature of the MOT, but was also to show how the temperature depends upon the size of the MOT and how the temperature varies as we change the detuning of the "cooling laser beam." The temperature of the cold atoms was found to be 261.66 µK while the temperature calculated by "Release and Recapture" was around 300 µK. The graphs showing different results are shown in figure 4.30.

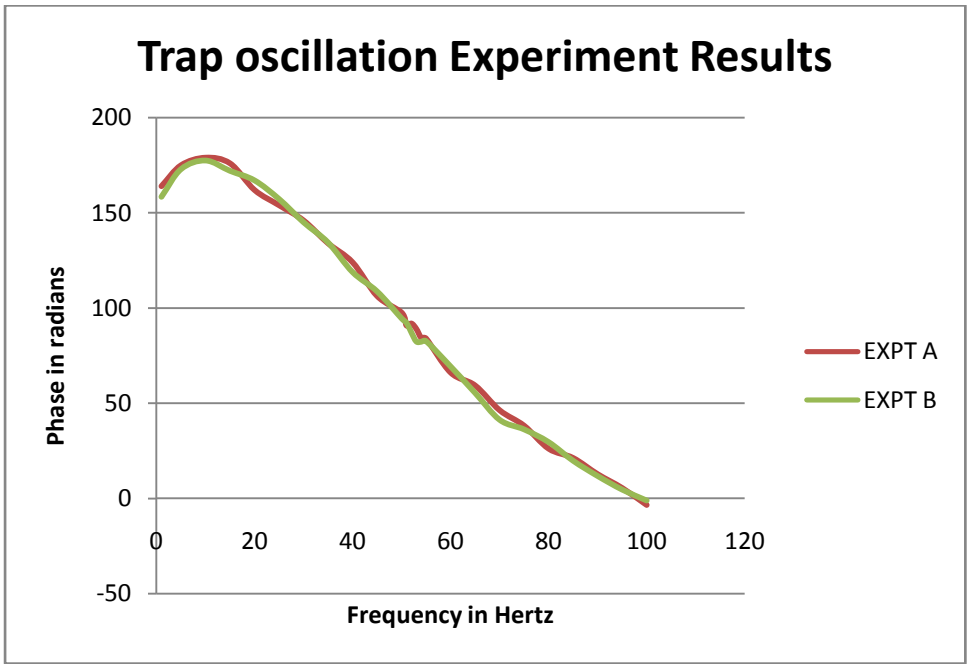

Fig. 4.30. Trap Oscillation experiment data

5. Experiment towards Single Photon Detection

5.1. Experimental Ideas and details:

Light matter interactions are studied with samples of single atom and single photon. To achieve single atom, Rubidium 87 atoms are laser cooled in a Magneto Optic Trap, and transferred to a magnetic trap. Detection of trapped atoms is usually done by illuminating the trap with a near resonant laser, and fluorescence is measured. Light matter interactions are studied by detecting the photons and obtaining the statistics of the arrival times of photon distribution.

5.2. Single-Photon Avalanche Diode (SPAD):

SPAD are a class of solid-state photo detectors based on a reverse biased p-n junction in which a photo-generated carrier can trigger an avalanche current due to the impact ionization mechanism. This device is able to detect low intensity signals (down to the single photon) and to signal the arrival times of the photons with a jitter of a few tens of picoseconds.

SPADs, like the avalanche photodiode (APD), exploit the photon-triggered avalanche current of a reverse biased p-n junction to detect an incident radiation. The difference between SPAD and APD is that SPADs are specifically designed to operate with a reverse bias voltage well above the breakdown voltage whereas APDs operate at a bias lesser than the breakdown voltage.

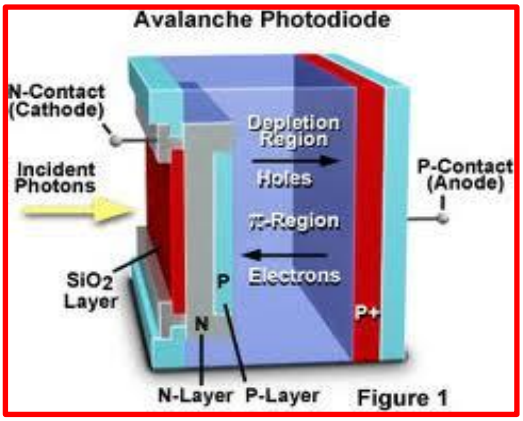

Fig. 5.1. Avalanche photodiode construction

In our experiments to detect single photons we are using single photon counting module SPCM-AQR-14 from Perkin Elmer [22]. The figure below show the same

Fig 5.2. SPCM-AQR-14 from Perkin Elmer

5.2.1. The features of SPCM-AQR-14 are[22]:

- It detects single photons of light over 400nm to 1060nm wavelength range
- Utilizes a unique silicon avalanche photodiode which has a circular active area whose peak photon detection efficiency over a 180 µm diameter exceeds 70% at 650 nm.
- Module can count to speeds exceeding 10 million counts per second(Mc/s)
- It has a "dead time" of 50 ns between pulses and Timing Resolution of 350 ps FWHM
- As each photon is detected, a TTL pulse, 35 ns wide is sent to output at the rear (BNC) connector
- Dark count: 100 counts/sec
- Supply voltage : + 5v/0.5A

Output of SPCM-AQR-14 measured on a oscilloscope:

- Pulse width ~ 20 ns
- Dead time of 50 to 70 ns between the pulses
- Pulse detection logic has to differentiate between a glitch and SPCM pulse
- Sampling time – resolution: 5ns

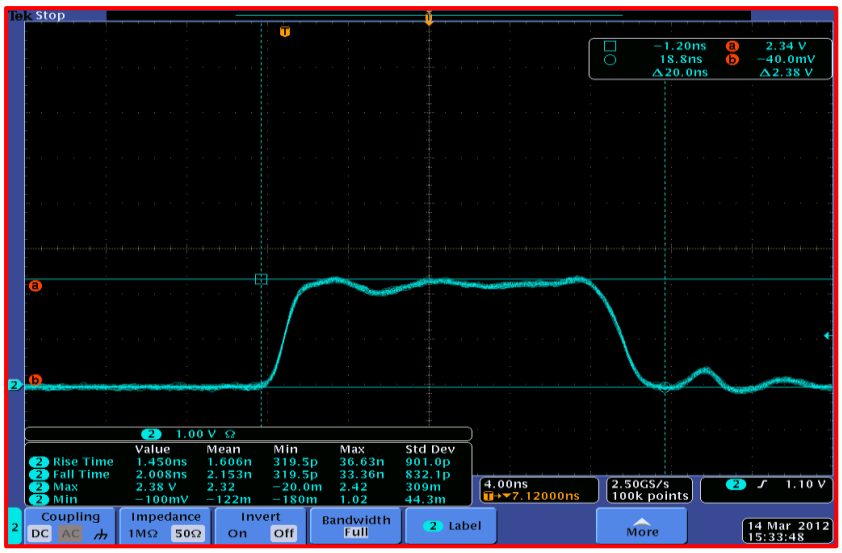

Fig 5.3. Output of SPCM-AQR-14 on oscilloscope

5.3. Level translator card for FPGA based Detection system:

For counting single photons, FPGA based Detection system is being developed by another group (Radio Astronomy Group). The FPGA board is a Virtex-5 board designed for high speed applications. It has 125MHz on-board clock, and 200MHz clock is generated internally. FPGA board is designed to accept Differential signalling – LVDS (Low voltage differential signalling)

A level translator card is required as interface between SPCM which gives out TTL signals and FPGA system which accepts differential signals.

5.3.1. LVDS (Low voltage Differential Signaling):

The LVDS standard is used in the applications in the data communications, tele- communications, server, peripheral, and computer markets where high-speed data transfer is necessary. LVDS offers a low cost, high speed, low power solution when compared to the other standards [23].

LVDS is defined in the TIA/EIA-644 standard. It is a low voltage, low power, differential technology used primarily for point-to-point and multi-drop cable driving applications. The standard was developed under the Data Transmission Interface committee TR30.2. It specifies a maximum data rate of 655 Mbps. Compared to other differential cable driv-

ing standards like RS422 and RS485, LVDS has the lowest differential swing with a typical voltage swing of 350 mV with a typical offset voltage of 1.25V above ground[23]. Different signal level comparisons are shown in figure 5.4.

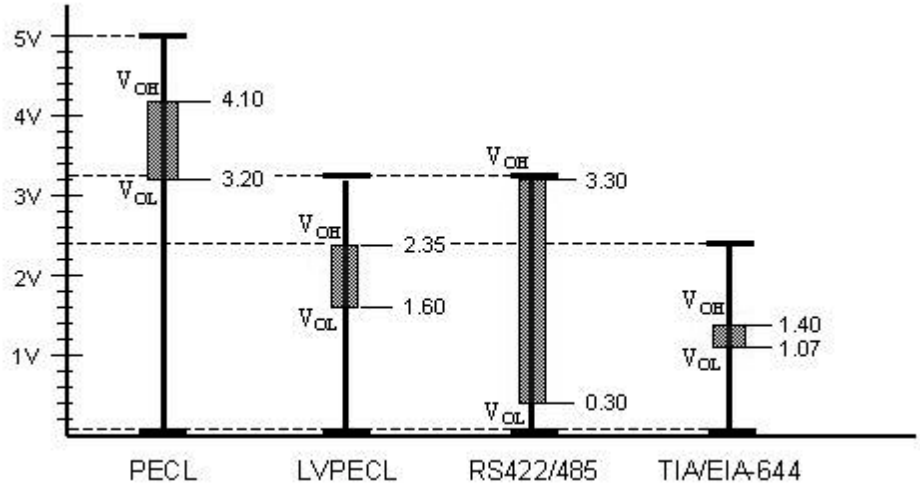

Fig 5.4. Signal level comparison

LVDS features a low swing differential constant current source configuration which supports fast switching speeds and low power consumption. This allows for other features not found in single ended technologies such as Common Mode Rejection.

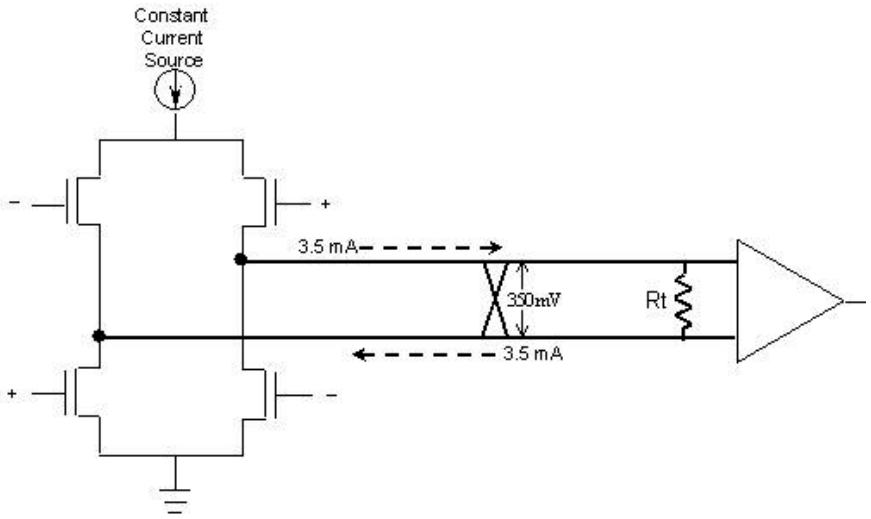

Fig 5.5. Driver/Receiver schematic of Differential Signaling

The advantages of Differential signaling over single ended technologies [23]:

1. It centers around 1.25Vwitha 350mv swing, and not dependent on the power supply voltage
2. Faster, stable signals and easier to migrate to lower power supply voltages.
3. Balanced differential lines have tightly coupled equal, but opposite polarity signals, which reduces the EMI.
4. Magnetic fields radiated by each of the conductor – gets cancelled.
5. Common mode rejection- Rejects any noise which is equally coupled on to the differential signals.

5.3.2. Level Translator (TTL to LVDS converter) Circuit

To achieve this we have designed a level translator card (figure 5.7) using IC DS90LV019[24], which is a Driver/Receiver designed specifically for the high speed, low power point-to-point interconnect applications. The block diagram of the setup is as shown in figure below. In our setup we are using two detectors SPCM A and B. The output of the two detectors are fed to the Level Translator (TTL to LVDS) converter.

DS90LV019 operates from a single 3.3V or 5.0V power supply and includes one differential line driver and one receiver [24].

The DS90LV019 features an independent driver and receiver with TTL/CMOS compatibility (DIN and ROUT). The logic interface provides maximum flexibility as 4 separate lines are provided (DIN, DE, RE, and ROUT). The driver has 3.5 mA output loop current. The driver translates between TTL levels (single-ended) to Low Voltage Differential Signalling levels. This allows for high speed operation, while consuming minimal power with reduced EMI. In addition, the differential signalling provides common-mode noise rejection.

The SPCM signals (TTL) of detector A and B which are converted into LVDS levels are sent to the FPGA board as shown in block diagram (figure 5.6). FPGA board is programmed to give the number of photons detected on each channel and the coincidence counting between the two detectors. Level Translator card has the provision to give out the triggering signals (TTL) to the gates of SPCM. This involved designing of pcb in ORCAD, assembly, testing of the pcb and module unit as shown in figure 5.8.

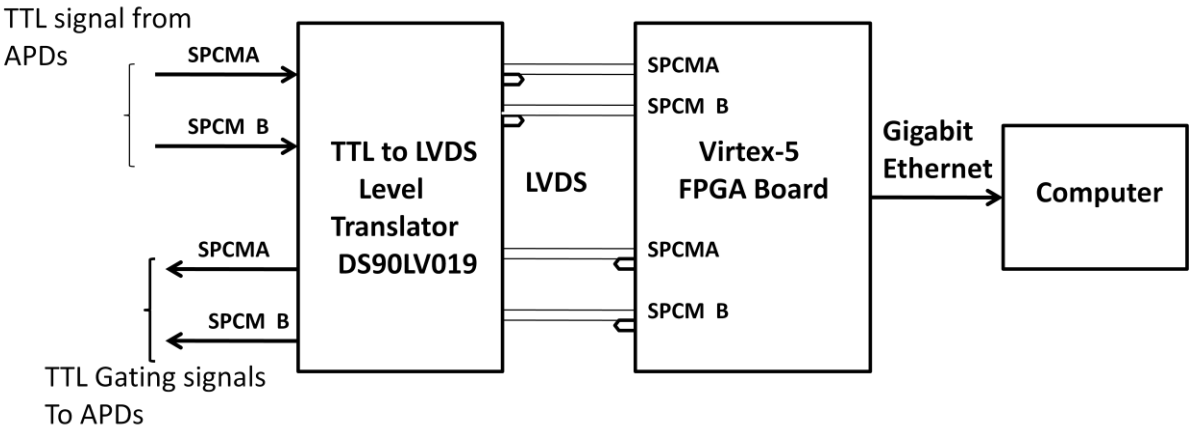

Fig 5.6. Block diagram of detection system using Level Translator and FPGA board

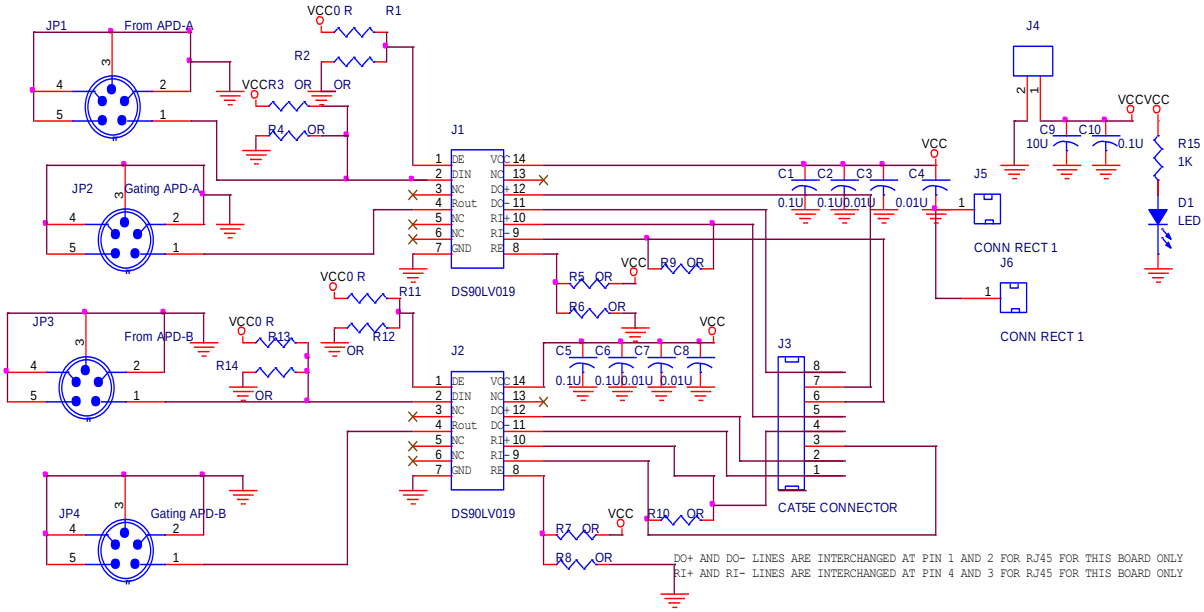

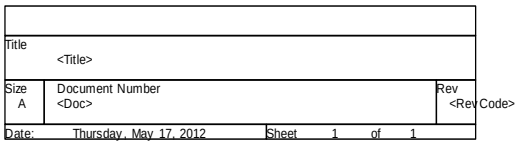

Fig 5.7. Schematic diagram of the Level Translator card

5.3.3. Results of the Level Translator Circuit

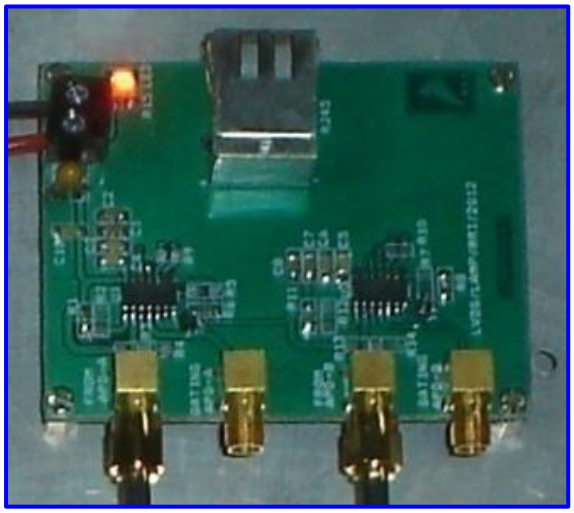

Fig 5.8. Level Translator card using DS90LV019

5.4. Coarse Delay circuit:

In single atom experiments two Avalanche Photo Detectors (APD) will be used to study the coincidence counting. In this process we have to vary or introduce the delay (up to few ns) in one of the Gating trigger signals given to the APD.

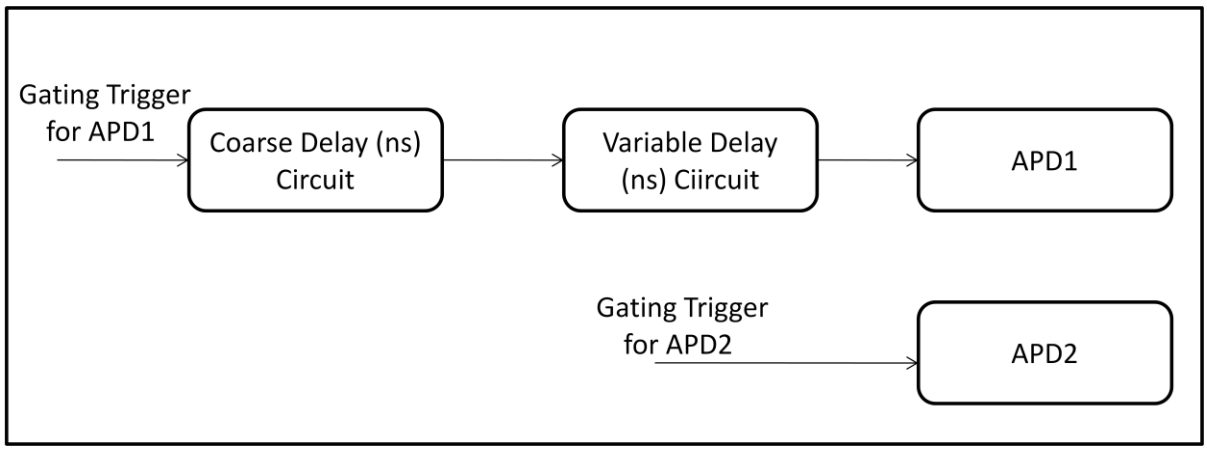

Fig 5.9. Block diagram of Setup of Single photon counting system

This is achieved in two stages:

a. Coarse Delay circuit- which introduces delay in steps of 10ns and

b. Variable delay circuit – 0 -10 ns variable delay.

Figure 5.10 gives the schematic of the Coarse Delay Circuit.

5.4.1. Schematic of Coarse delay (ns) circuit:

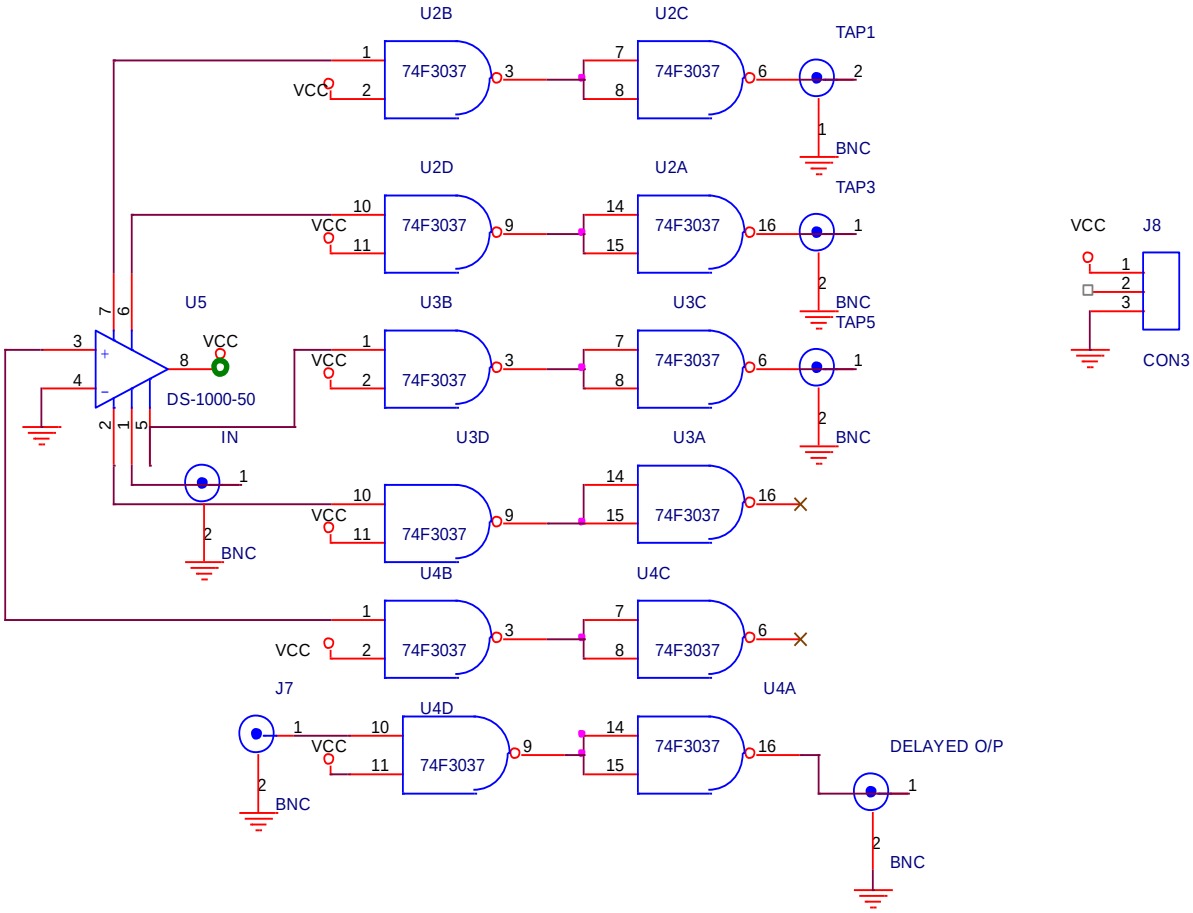

Fig 5.10. Schematic diagram of Coarse Delay unit

5.4.2. IC DS-1000-50-series Delay Lines

This circuit has two stages. First stage consists of DS-1000 (U5) series chip from Dallas semiconductors. The DS1000 series delay lines have five equally spaced taps providing delays from 4 ns to 500 ns. These devices are offered in a standard 14-pin DIP that is pin-compatible with hybrid delay lines. The features of DS-1000 series chips are [25]:

*All-silicon time delay

* 5 taps equally spaced

* Delays are stable and precise

* Both leading and trailing edge accuracy

* Delay tolerance ±5% or ±2 ns, whichever is greater

* Low-power CMOS

* TTL/CMOS-compatible

* Custom delays available

* Fast turn prototypes

The DS1000 series delay lines provide a nominal accuracy of ±5% or ±2 ns, whichever is greater. The DS1000 5-Tap Silicon Delay Line reproduces the input logic state at the output after a fixed delay as specified. The DS1000 is designed to reproduce both leading and trailing edges with equal precision. The pin-out details of the DS-1000-50 is given in the figure5.11. It has one IN pin, and 5 output taps which give delays from 10 ns to 50 ns.

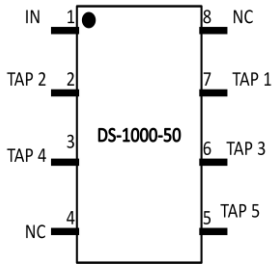

Fig 5.11: Pin out details of IC DS-1000-50

The logic diagrams of DS-1000-50 IC is given below

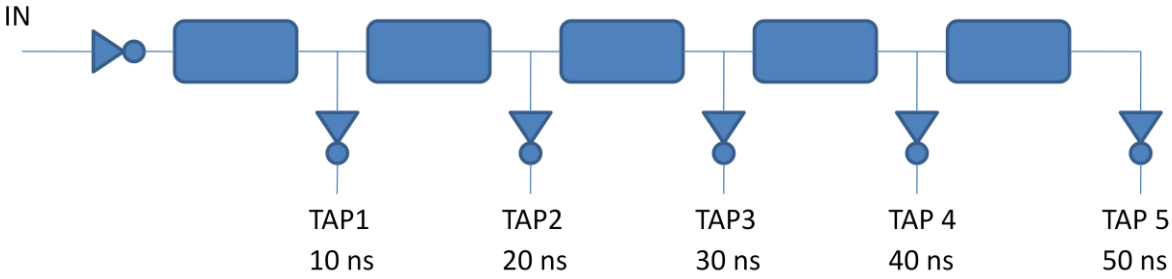

Fig 5.12 : Logic diagram of IC DS-1000-50

The second stage of the circuit is Line driver IC 74f3037[26], which is a high current line driver composed of four 2–input NAND gates. It is used to overcome the transmission line effects of PC boards which appear when fast edge rates are used. The drive capability of the 74F3037 is 67mA source and 160mA sink with a VCC as low as 4.5V. This guarantees incident wave switching with VOH not less than 2.0V and VOL not more than 0.8mA while driving impedances as low as 30 ohms.

Features of 74f3037 [26] are:

- 30Ω line driver
- 67mA output drive capability in the high state
- High speed
- Facilitates incident wave switching

• 3nh lead inductance each on VCC and GND when both side pins are used

• 160mA output drive capability in the low state

Each output (TAP1 to TAP5) of DS-1000-50 is connected through two NAND gates of 74f3037, as they have to be connected to the APD trigger inputs which are a 50 ohm input. In the front panel of the module we have made provision for selection of 10ns, 20 ns and 30 ns delays with a rotary switch.

5.5. Variable delay circuit:

Coarse delay circuit is followed by a Variable Delay circuit [27]. Along with the coarse delay variation in the steps of 10 ns, we need to have a provision for variable delay (1 to 10 ns). The block diagram for the Variable delay circuit is shown in figure 5.13.

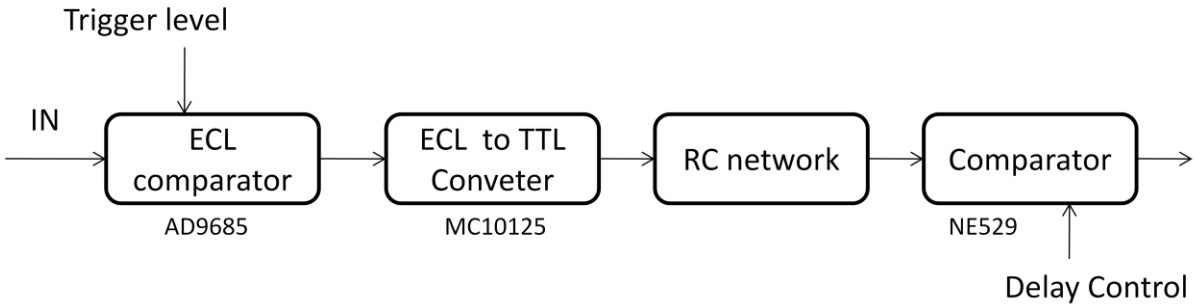

Fig 5.13: Block diagram of Variable Delay Circuit

5.5.1. ECL comparator (AD9685)

The IN signal is the output of the Coarse Delay module which is delayed by 10, 20 or 30 ns, depending on the selection switch on the front panel. The input signal is first fed to the ECL comparatorU1 AD 9685 (figure 5.14), which converts the input signal to ECL levels (-2V). IC AD9685 is a high speed comparator with a propagation delay of 2.7ns. Output stage can drive a load of 50 ohms terminated transmission line, with 30ma of output drive capacity. Trigger level in our circuit is set a fixed voltage reference. For more precise control we can use 12 bit DAC to improve the accuracy.

5.5.2. ECL to TTL converter (MC10125)

The comparator's output is fed to MC10125 which is ECL to TTL converter. The MC10125 is a quad translator for interfacing data and control signals between the MECL section

and saturated logic sections of digital systems. The MC10125 incorporates differential inputs and Schottky TTL "totem pole" outputs. Power supply requirements are ground, +5.0 Volts and –5.2 Volts. Propagation delay of the MC10125 is typically 4.5 ns [28].

The MC10125 has fanout of 10 TTL loads. The dc levels are MECL 10,000 in and schottky TTL, or TTL out. This device has an input common mode noise rejection of ± 1.0 Volt. An advantage of this device is that MECL level information can be received, via balanced twisted pair lines, in the TTL equipment. This isolates the MECL logic from the noisy TTL environment. MC1025 converts the ECL output of comparator into a TTL (+5V) pulse.

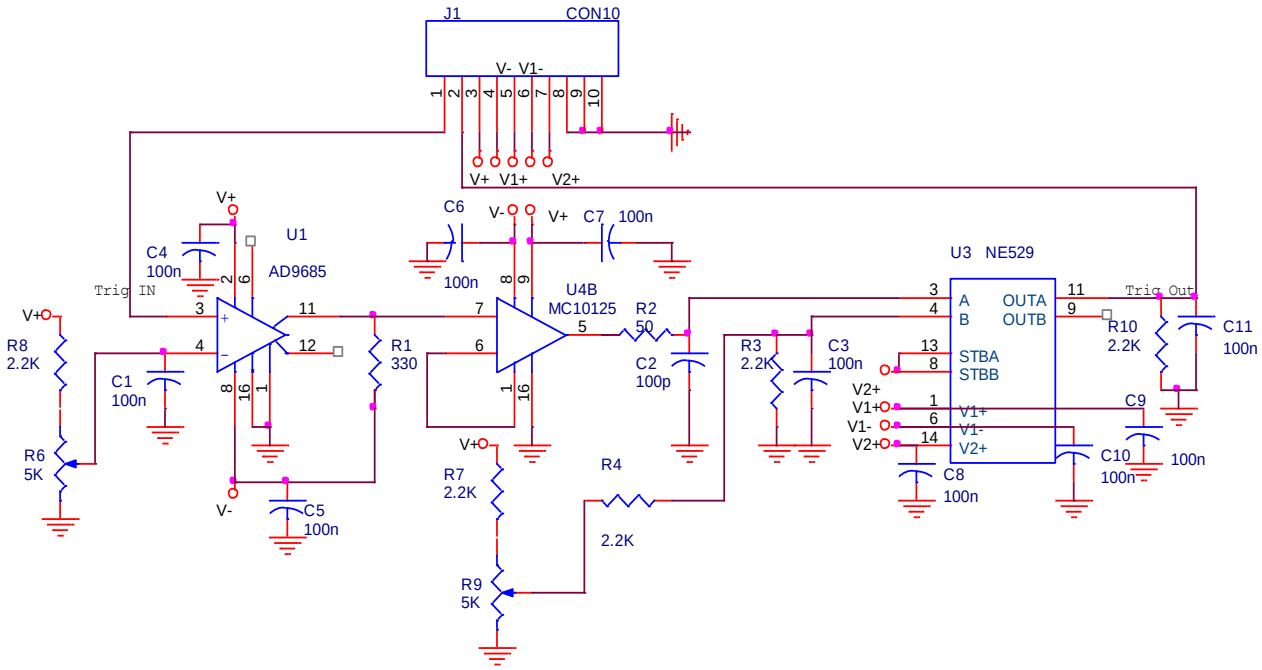

Fig 5.14 : Schematic diagram of Variable Delay Circuit

The output of the MC10125, a TTL +5V pulse is fed through RC network R2-C2 (R=50 ohms, C= 100P) to NE529 (U3) which is a second comparator stage.

5.5.3. High-speed analog voltage comparator (NE529)

The NE529 is a high-speed analog voltage comparator which combines Schottky diode technology with the conventional linear process. This allows simultaneous fabrication of high-speed TTL gates with a precision linear amplifier on a single monolithic chip [29].

Features of NE529

- 10 ns propagation delay
- Complementary output gates
- TTL or ECL compatible outputs
- Wide common-mode and differential voltage range
- Typical gain 5000

APPLICATIONS

- A/D conversion
- ECL-to-TTL interface
- TTL-to-ECL interface

Input A of NE529 is the TTL output from MC10125 fed through R2-C2 network. The effect of the RC network is to slower the rise time of rising edge of the pulse to approximately 10 nanoseconds. Input B is the comparison level (0 – 5V), variable with R4,R7 and R9 network(called as Delay control in block diagram 5.13). This voltage controls the time at which the input pulse reaches the required level and with it the delay between the trigger pulse and the output of the comparator NE529. For future requirements we are planning to have D-A converters, so that digital control of the delay can be achieved.

The final trigger out is the delayed pulse which is given to the gate trigger of the APD detector. Both the circuits i.e. Coarse delay circuit and Variable delay circuit are combined into one unit, with front panel controls. The complete unit of Delay module is shown in fig 5.15.

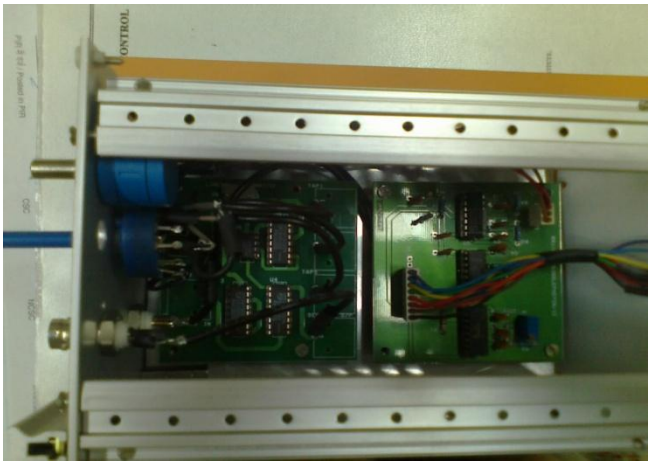

Fig 5.15 :Delay circuit module

5.6. Results of Coarse ad Delay circuit:

The following figures shows the output result of the Delay unit. Ch1 is the input signal from a reference source, and ch2 is the ouput signal of the module. The different values of delays are achieved by the selection switch and potentiometre (R9) on the front panel. The following figures 5.16 to 5.18 indicates diffenerent (delta) delay values of 32ns, 42ns and 67 ns.

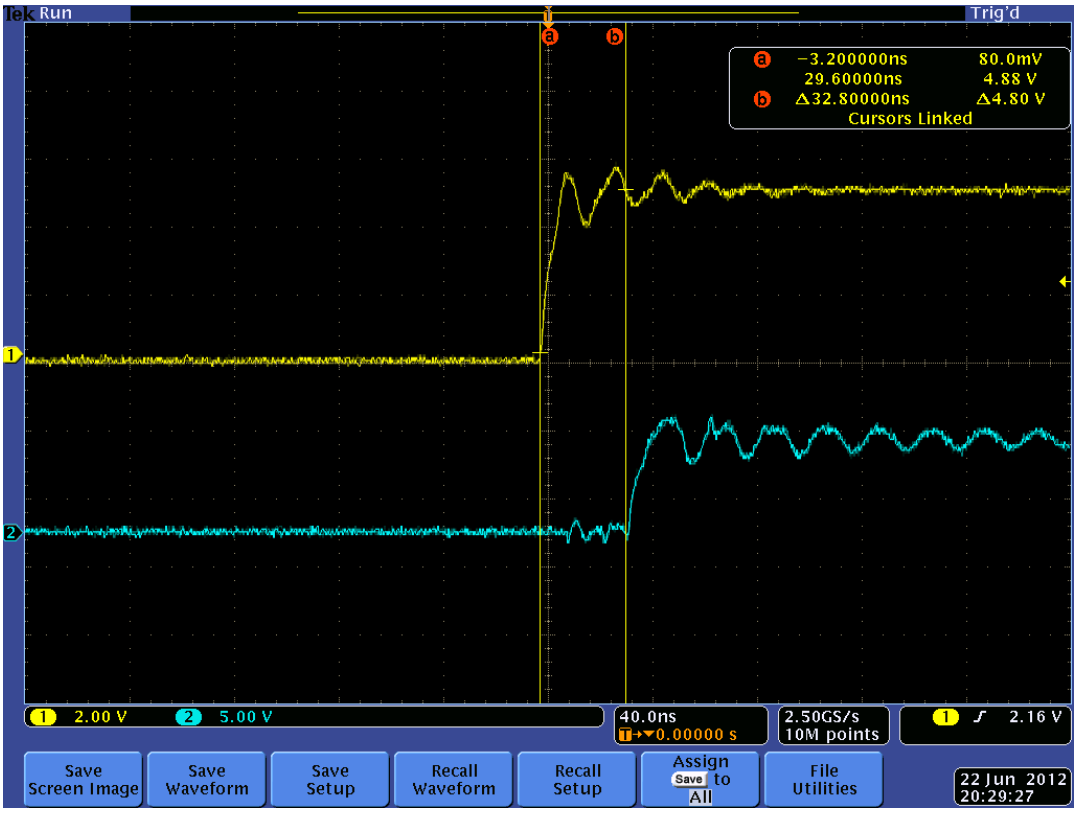

Fig 5.16 Output signal delayed by 32ns

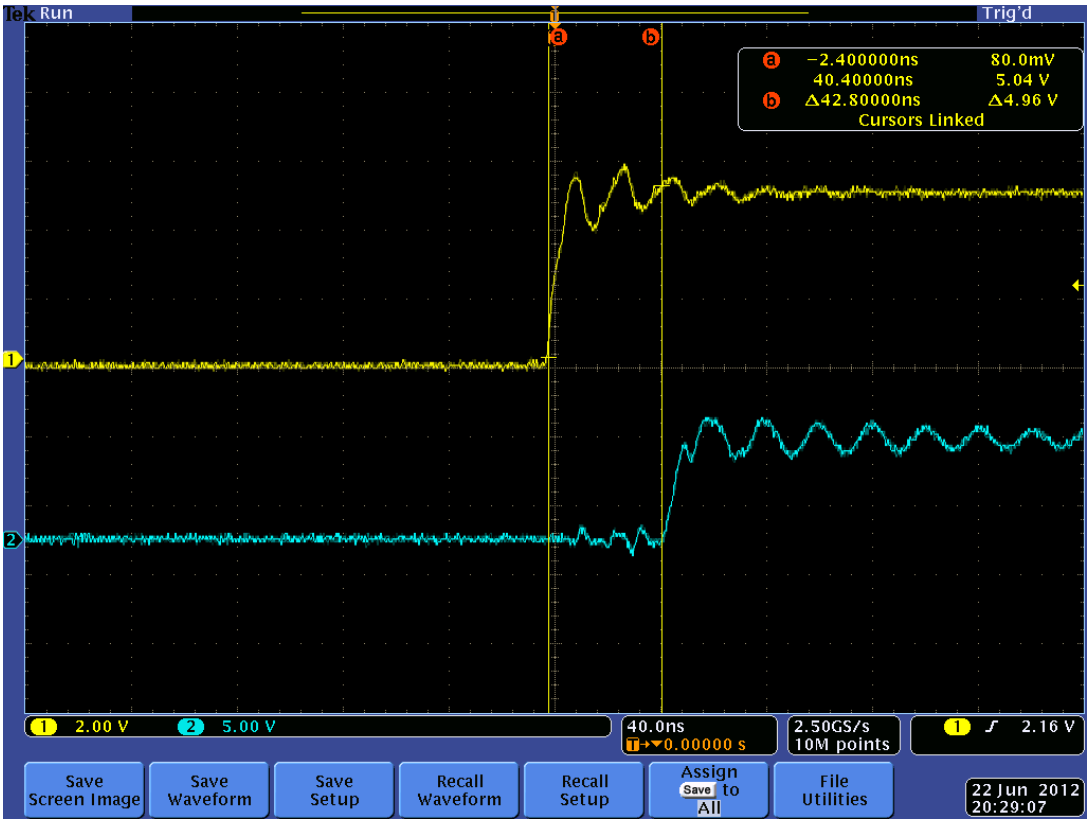

Fig 5.17. Output signal delayed by 42ns

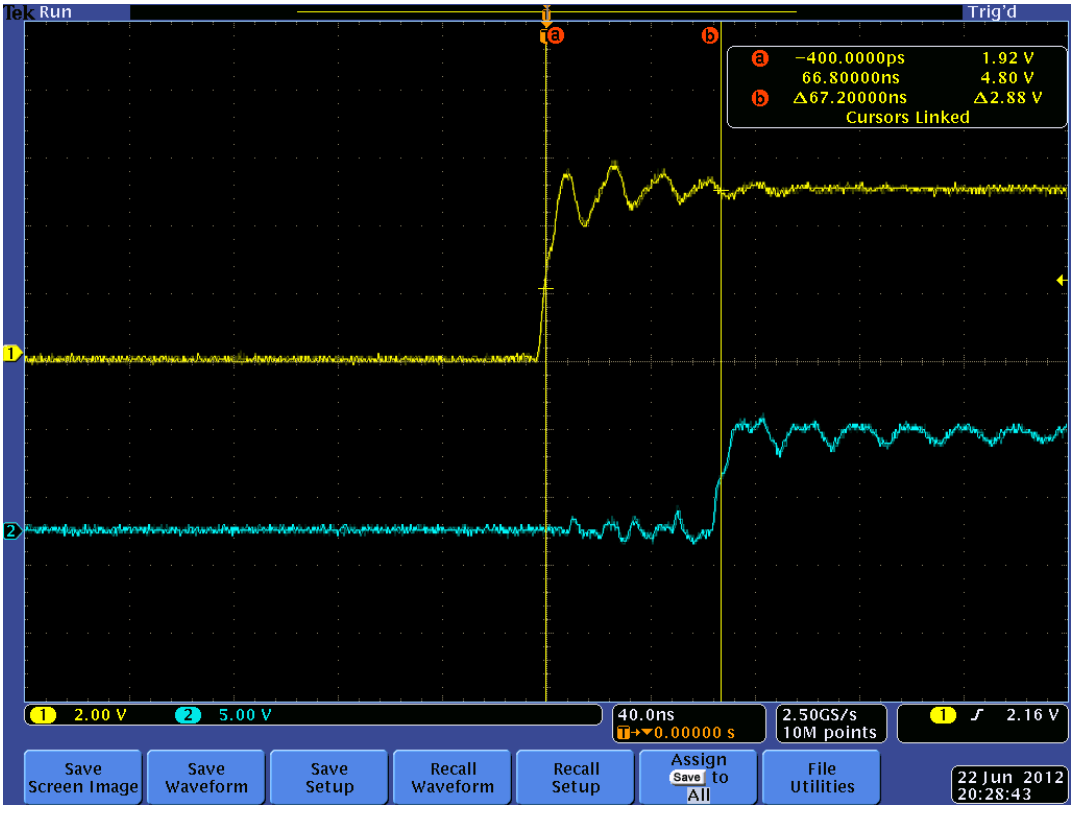

Fig 5.18. Output signal delayed by 67ns

Chapter 6 Summary and Conclusions

6.1. Summary

The present study was focused on the development of Electronic circuits, modules, instrumentation and automation of the experiment towards measurement of Ultra cold atoms in Laser cooling Lab at Raman Research Institute.

The important requirements of a Laser cooling and atom trapping experiments are:

1. Stable Laser Sources
2. Vacuum systems
3. Magnetic coils and switching circuits
4. Measurement Techniques for precision measurement of MOT (Magneto Optic Trap) parameters.
5. Automation of the experiments
6. Imaging Techniques for imaging the Magneto Optic Trap (MOT)

The present work is aimed towards achieving the few requirements of the Laser cooling experiments.

To achieve a stable Laser source, Laser diode is placed in an External Cavity Diode Laser (ECDL) to achieve laser sources stable upto few MHz. The components of an ECDL and Temperature stabilization circuits and Frequency Locking Techniques have been discussed.

The laser frequency (at 10^{14} Hz) has to be shifted by a few hundred MHz using Acousto Optic modulators (AOM). A PI based feedback mechanism is developed and implemented to control any error produced due to the shift in the RF output of an AOM,which is detected and relevant control action is taken by sending a feedback signal back to the AOM.

To achieve the MOT (Magneto Optic Trap) and characterize the MOT parameters, IGBT based switching system is designed and developed which switches the magnetic coils on and off at currents up to 5A, up to 100 Hz to trap the atoms. To automate the experi-

ment LabVIEW based programs are written and integrated with the Magnetic coil switching circuit, to vary the currents in few milli seconds of time intervals. To measure the temperature of the Magneto Optic Trap (MOT), Lock-in detection based technique known as Trap Oscillation method is designed and developed.

Towards Single Atom detection Level Translator circuit, Coarse delay circuit and Variable Delay circuit have been designed and developed.

6.2. Conclusions

Based on the study carried out the following broad results and conclusions are discussed:

1. The frequency drifts we have observed in few models of AOM vary from 0.4MHz to 0.9MHz. Based on these values, we have designed the system to control the drifts upto +/- 1.5 MHz, making provision for any spurious drifts. This mechanism stabilizes the absolute frequency output of the AOM with an accuracy upto few KHz. This method will be useful in situations where the AOM driver voltage is not very stable and faster and stable control of the output frequency is desired. +/- 1.5MHz window gives a stability of one part in 10 million in the laser frequency

This work was presented as a paper titled

“Feedback control Mechanism for Acousto-Optic Modulator”,

M S Meena , V Arun, SahilSanan and Andal Narayanan

has been published in Instrumentation Society of India (ISOI), IISC, Bangalore in Decem

ber 2010 issue.

(JL. of Instrum.Soc. Of India, Vol. 40 No. 4 , December 2010).

2. To study the quantum walk of light in frequency space, it was required to introduce phase noise in the Versatile Function generators (VFG), which we achieved using Lab-VIEW programs, which enabled us to introduce systematic phase noise between signal generators which were used to drive the AOMs. This work resulted in interesting results which was published in **Physical Review A, Phys. Rev. A 84, 042322 (2011) titled** "**Quantum walk of light in frequency space and its controlled dephasing**" , Deepak Pandey, NandanSathpathy, Meena M.S. and HemaRamachandran.

3. To capture the atoms in a Magneto-Optic Trap, the magnetic field needs to be switched on. For characterising the MOT, i.e. to calculate number of atoms, decay rate etc, it is essential to switch off the MOT. A IGBT (Mitsubishi) based a switching system is developed and implemented which switches the magnetic coils on and off at currents up to 5A, up to 100 Hz. IGBT based system includes driver circuitry for IGBT, snubber circuit for protections purposes, and freewheeling circuitry for back emf suppressions. The currents in magnetic coils are ramped up and down in time intervals of few milliseconds, as per the experimental requirements. Data Acquisition systems from National Instruments and LabVIEW programs are designed, developed and implemented to automate the experiments for switching the magnetic coils on/off and for ramping the currents in the magnetic coils. Rise time of about 7ms and fall time of 16ms are achieved after tuning the RLC parameters of the freewheeling circuit.

4. To measure the temperature of the Magneto Optic Trap (MOT), Lock-in detection based technique known as Trap Oscillation method is designed and implemented. An additional pair of magnetic coils is used, which are driven by a Power amplifier (OPA 541) to introduce oscillating magnetic field. This oscillating magnetic field causes the cold atom cloud to oscillate, which is detected by a detector. Lock-in detection techniques are used measure the phase difference (Ø) between the reference signal and the detector signal. By measuring the phase difference (Ø), at different frequencies of the oscillating magnetic field, the temperature of the cold cloud is evaluated as 260 µ Kelvin.

5. In our experiments to detect single photon we are using single photon counting module SPCM-AQR-14 from Perkin Elmer. For counting single photons, FPGA based Detection system is used. It is a Virtex-5 board, has 125MHz on-board clock. FPGA board is designed to accept Differential signalling – LVDS (Low voltage differential signalling). A level translator card is required as interface between SPCM which gives out TTL signals and FPGA system which accepts differential signals. To achieve this level translator card using IC DS90LV019, is designed and implemented, which is a Driver/Receiver designed specifically for the high speed low power point-to-point interconnect applications.

6. In single atom experiments two Avalanche Photo Detectors (APD) are used to study the coincidence counting. In this process we have to vary or introduce the delay (up to few ns) in one of the Gating trigger signals given to the APD. To achieve this a module having(a) Coarse Delay circuit which introduces delay in steps of 10ns and (b) Variable delay circuit for 0 -10 ns variable delay are designed, tested and implemented.

6.3. Scope for Further Studies

Laser cooling and atom trapping is challenging field in experimental physics. As the new experiments are designed, the experimental techniques and requirements would change. The following points can be thought of as requirement for future studies

1. We have implemented PI based Lock-in circuits for locking the lasers to hyperfine transitions. A DSP (Digital Signal Processing) based Lock-in circuits can be designed and implemented for efficient Locking of Lasers.

2. For Bose-Einstein condensation experiments, which can be considered as extension of Laser cooling experiments, laser cooled atoms in a MOT will be transferred to a Magnetic Trap. The magnetic field gradients will be much higher, and would require magnetic coil carrying currents upto 25 A. The switching circuits at such high currents require much more complex and fast switching circuitry.

3. As Atom-chip BEC experiments require control signals in the order of microsecond to few milli seconds, so a real time system will be essential. Compact RIO is a real-time module from National Instruments with FPGA programmable Chassis and controller. The complete switching sequence for the BEC control program can be designed with Compact RIO, I/O modules and LabVIEW.

4. We are aiming towards achievement of single atom and single photon in our lab. The presently existing Virtex-5 FPGA system with level translator card for Single atom analysis, can be used systematically used to carry out further investigations.

References:

[1] K. Razdan. D and A.VanBaak, "Demonstrating optical beat notes through heterodyne experiments" Department of Physics and Astronomy, University of Wisconsin and Department of Physics and Astronomy, Calvin college, Am.J.Phys. 70(10), October 2002.

[2] H.J.Mains and P.J.Manson "The stabilization and scanning of Dye Laser using a Feedback Servo-System", Department of Physics, University of Otago.

[3] L.Holberg, R.Drullinger and B.Dahmani, "Frequency stabilization of semiconductor laser by resonant optical feedback", National Bureau of Standards, Boulder, Colorado, OPTICS LETTERS, Vol.12, No.11, November 1987.

[4] I. Shavarchuck, K.Dieckmann, M.Zielonkowski, J.T.M. Walraven, "Broad-area diode laser system for a rubidium Bose-Einstein condensation experiment", Applied Physics B,71(4): 475-480, 2000

[5] "Understanding Mixers", http://www.minicircuits.com/pages/pdfs/mixer1-2.pdf, Jan 2007.

[6] Filter design: http://www.ecircuitcenter.com/Circuits/opsalkey1/opsalkey1.htm

[7] VFC 32 Design: http://focus.ti.com/docs/prod/folders/print/vfc32.html

[8]http://www.mitsubishielectric.com/semiconductors/files/manuals/powermos3_0.pdf

[9]http://www.mitsubishielectric.com/semiconductors/files/manuals/powermos4_0.pdf

[10] www.agilent.com

[11] Jeffrey Travis, Internet Applications in LabVIEW, Prentice Hall, NJ 07458, 2000.

[12] Wells, Lisa & Jeffery Travis, LabVIEW for Everyone, Prentice-Hall, New Jersey, 1996

[13] www.ni.com/data-acquisition

[14] http://sine.ni.com/ds/app/doc/p/id/ds-22/lang/en

[15] "Design of low-voltage, low-power operational amplifier cells", By Ron Hogervorst, Johan H. Huijsing

[16] R.S. Bunven."Kilowatts on Order (Power Amplifiers)," IEEE Spectrum.February 1993. Vol.30 Iss.2., pp. 32-37

[17] Stanley, G.R; Bradshaw, K.M.; "Precision DC-AC power conversion by optimization of the output current waveform the half bridge revisited," IEEE Trans. on Power Electronics. Vol. I4 Iss.2 ,March 1999, pp.372 –380

[18] www.datasheetarchive.com/OPA541

[19]www.signalrecovery.com

[20] http://electron9.phys.utk.edu/optics507/modules/m10/tn1000.pdf

[21] http://www.thinksrs.com/downloads/PDFs/ApplicationNotes/AboutLIAs.pdf

[22] http://www.scitecinstruments.pl/detektory/pcm/pdf/SPCMAQR.pdf

[23] http://www.fairchildsemi.com/an/AN/AN-5017.pdf

[24]http://www.ti.com/lit/ds/symlink/ds90lv019.pdf

[25]http://www.datasheetcatalog.org/datasheets2/67/67189_1.pdf

[26]http://www.nxp.com/documents/data_sheet/74F3037.pdf

[27] John Z person, An externally triggered circuit producing digitally controlled delays with sub- nanosecond step size, Meas. Sci. Technol.1(1990)24-28

[28]http://www.datasheetcatalog.org/datasheet/on_semiconductor/MC10125-D.PDF

[29] http://www.datasheetcatalog.org/datasheet/philips/NE529_2.pdf

APPENDIX

DATA SHEETS